

Revealing SARS-CoV-2 Functional Druggability Through Multi-Target Cadd Screening of Repurposable Drugs

Yash Gupta^{1,2}, Dawid Maciorowski^{1,3}, Raman Mathur¹, Catherine M Pearce¹, David J. Ilc^{1,3}, Hamza Husein^{1,3}, Ajay Bharti⁴, Daniel P. Becker³, Brijesh Rathi^{2,5}, Steven B Bradfute⁶, Ravi Durvasula^{1,2}, Prakasha Kempaiah^{1,2*}

1 Loyola University Chicago Stritch School of Medicine, Chicago, IL, 60153, USA; **2** Department of Medicine, Loyola University Medical Center, Chicago, IL, 60153, USA; **3** Loyola University Chicago, Chicago, IL, USA; **4** Division of Infectious Diseases, Department of Medicine, University of California, San Diego, CA, 92093, USA; **5** Laboratory for Translational Chemistry and Drug Discovery, Hansraj College, University of Delhi, India; **6** Center for Global Health, Division of Infectious Diseases, Department of Internal Medicine, University of New Mexico, Albuquerque, New Mexico, USA.

Number of Tables: 10; Number of Figures: 16

ABSTRACT: The emergence of SARS/MERS drug resistant COVID-19 with high transmission and mortality has recently been declared a deadly pandemic causing economic chaos and significant health problems. Like all coronaviruses, SARS-CoV-2 is a large virus that has many druggable components within its proteome. In this study, we focused on repurposing approved and investigational drugs by identifying potential drugs that are predicted to effectively inhibit critical enzymes within SARS-CoV-2. We shortlisted *seven* target proteins with enzymatic activities known to be essential at different stages of the virus life cycle. For virtual screening, the energy minimization of a crystal structure or modeled protein was carried out using Protein Preparation Wizard (Schrödinger LLC, 2020-1). Following active site selection based on data mining and COACH predictions, we performed a high-throughput virtual screen of drugs (n=5903) that are already approved by worldwide regulatory bodies including the FDA, using the ZINC database. Screening was performed against viral targets using three sequential docking modes (i.e. HTVS, SP and XP). Our *in-silico* virtual screening identified ~290 potential drugs based on the criteria of energy, docking parameters, ligand and binding site strain and score. Drugs specific to each target protein were further analyzed for binding free energy perturbation by molecular mechanics (prime MM-GBSA) and pruning the hits to the top 32 candidates. A top lead from each target group was further subjected to molecular dynamics simulation (MDS) using the Desmond module to validate the efficacy of the screening pipeline. All of the simulated hit-target complexes were predicted to strongly interact and with highly stable binding. Thus, we have identified a number of approved and investigational drugs with high likelihood of inhibiting a variety of key SARS-CoV-2 proteins. Follow-up studies will continue to identify inhibitors suitable for combination therapy based on drug-drug synergy to thwart resistance. In addition, the screening hits that we have identified provide excellent probes for understanding the binding properties of the active sites of all seven targets, further enabling us to derive consensus molecules through computer-aided drug design (CADD). While infections are expanding at a rampant pace, it must be recognized that resistance will grow commensurately through either genetic shift and/or genetic drift to all small molecule drugs identified. Vaccines should provide a more permanent solution through prevention, but resistivity is still a possible scenario. Nevertheless, a persistent multi-target drug development program is essential to curb this ongoing pandemic and to keep reemergence in check.

Key Words: SARS-CoV-2, COVID-19, CADD, virtual screening, approved drugs, drug repurposing, essential targets, molecular docking, molecular dynamics simulations

Address correspondence to: **Prakasha Kempaiah**, Ph.D, Loyola University Chicago Stritch School of Medicine, Chicago, IL- 60153,USA, e-mail: Pkempaiah@luc.edu

ABBREVIATIONS: COVID-19 (CoronaVirus Disease-2019); Severe Acute Respiratory Syndrome (SARS); Middle Eastern Respiratory Syndrome (MERS); computer-aided drug design (CAAD); PIPPro (Papain-like proteinase); 3-Chymotrypsin-Like Protease (3CLpro); RNA-directed RNA polymerase (RdRp); Nonstructural Uridylate-specific endoribonuclease (NendoU); exoribonuclease (ExoN); 2'-O-methyltransferase (2'-O-MT); mechanism of action (MOA); high through put virtual screening (HTVS); COACH- Meta-server approach to protein-ligand binding site prediction

INTRODUCTION. A novel coronavirus was first reported in Wuhan, the capital city of the Hubei province in China in December of 2019¹. This pathogen has been named SARS-CoV-2² and the disease caused by it, COVID-19 (Coronavirus Disease-2019). Epidemiological investigations have suggested that the source of the outbreak was associated with a market that sells various live animals¹. The epicenter of the outbreak quickly changed from China to the Europe and United States. Subsequently, SARS-CoV-2 outbreak was declared a pandemic by the World Health Organization (WHO), as this deadly and highly infectious virus continues to propagate around the globe. It has now (May 8th, 2020) spread to more than 188 countries, infecting at least 3.93M people, and killing 274,422^{3,4}. The pathogen spreads rapidly from person-to-person in familial, clinical, and community settings^{5,6}. Common symptoms include fever, cough, shortness of breath, diarrhea and fatigue, to more severe symptoms including atypical pneumonia^{1,7}.

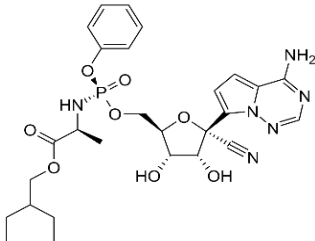
The tactical approach to studying and understanding this virus comes at the familial level. SARS-CoV-2 is a member of the *Coronaviridae* family. There are two other highly pathogenic coronaviruses that have significantly affected the human population which include SARS-CoV that causes Severe Acute Respiratory Syndrome (SARS), and MERS-CoV, which causes Middle Eastern Respiratory Syndrome (MERS). The first known case of SARS occurred in November of 2002 in China from where it quickly spread throughout mainland China and various other countries including Canada and Vietnam⁸. Eventually, there were 8,096 reported cases with 774 deaths in 27 countries affected by the SARS epidemic⁹. After SARS, the outbreak of MERS in 2012 marked the second time in very recent history that a highly pathogenic coronavirus was introduced to humans¹⁰. Although not as infectious as SARS, causing only 1,728 reported cases, MERS was extremely lethal, causing 624 deaths¹¹. A critical epidemiological characteristic that both SARS and MERS share their severe effect on healthcare workers. At an early point during the SARS epidemic, one-third of the population affected by this virus was healthcare providers⁸. In May of 2015, a MERS outbreak in South Korea exhibited significant nosocomial transmission involving 16 hospitals and 186 patients, all traced to a single individual returning from the Middle East¹². In fact, nosocomial transmission of these two viruses is strongly evident, as 40-100% of MERS and SARS cases were linked to clinical settings^{13,14}. The current COVID-19 situation is evolving rapidly with great concerns regarding nosocomial transmission resulting in unmanageable strain on the healthcare system^{6,15}. The nosocomial transmission evident in both MERS and SARS was linked to viral shedding associated with symptomatic disease that occurred when patients sought medical care¹⁶⁻¹⁹. Importantly, in the case of SARS-CoV-2, transmission can occur in asymptomatic infection and with varied viral loads^{15,20}. Furthermore, SARS-CoV-2 has been detected in blood, as well as in oral and anal specimens, suggesting that it can be shed in various body fluids resulting in transmission through respiratory droplets and through fecal-oral transmission⁷.

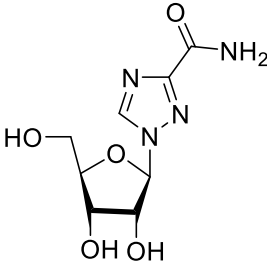
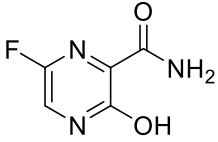
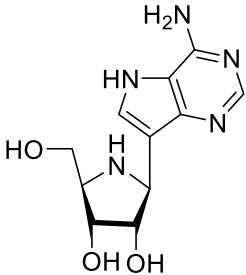
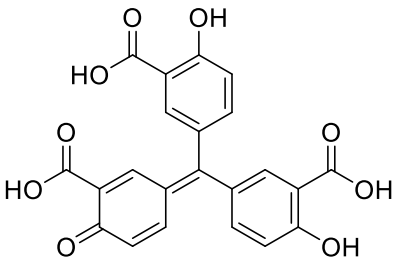
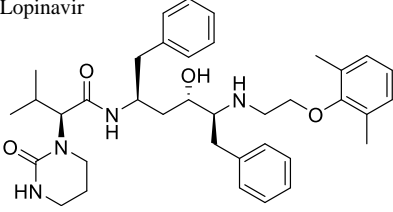
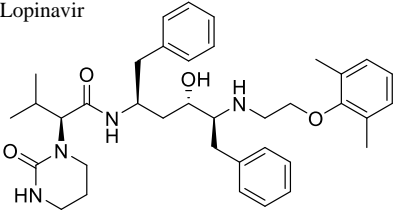
The genome of coronaviruses consists of a single stranded, positive sense RNA, causing respiratory and enteric disease in mammals including humans. This family of viruses consists of a large genome, ranging from 28 to 32 kilobases²¹. Coronavirus family members are organized into three subsets based on antigenic and genetic facets: α -CoVs, β -CoVs, and γ -CoVs^{22,23}. MERS-CoV, SARS-CoV, and SARS-CoV-2 are all β -coronaviruses, where both SARS-CoV and MERS-CoV are derived from a the lineage B and MERS-CoV is derived from the lineage C β -coronavirus²⁴. Interestingly, these viruses have similar genomic structures with functional proteins encoded at the 5' end, and structural proteins encoded at the 3' end of the genome²⁵. β -Coronaviruses have accessory proteins dispersed throughout their structural genes with both SARS-CoV and SARS-CoV-2 having seven different accessory proteins, while MERS-CoV has five different accessory proteins^{21,25}.

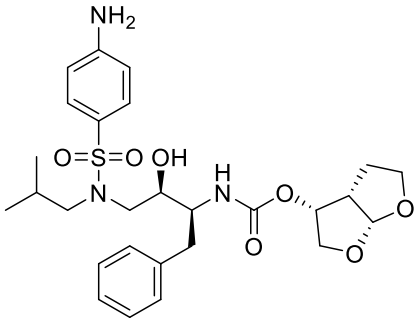
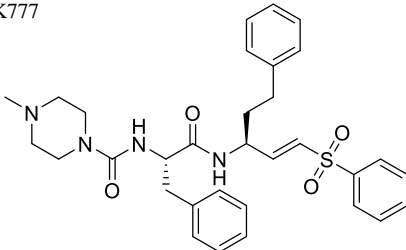
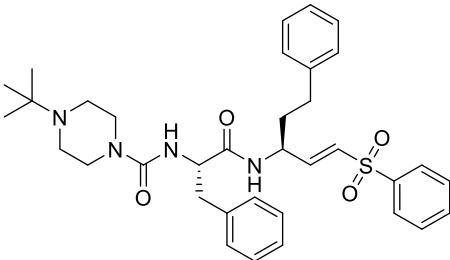
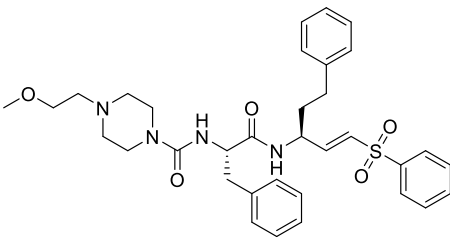
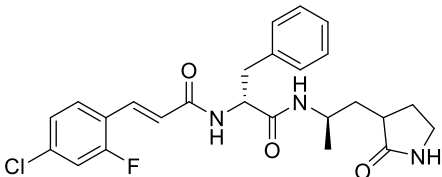
Currently, there is no approved treatment for COVID-19 and there is a critical need to identify effective agents against it. The discovery and development of novel compounds that specifically target SARS-CoV-2 will require an extended period of preclinical testing before they can enter clinical trials. Due to limited time, there is an urgent need for faster treatment options. One approach is through screening already approved drugs in libraries that could be repurposed for SARS-CoV-2. In this study, we have used a multi-pronged drug discovery approach through advanced screening that is in line with the World Health Organization's (WHO) guidance to repurpose approved drugs with demonstrated acceptable safety profiles. As potential new treatments are identified, mechanistic and clinical studies can be immediately performed to determine the efficacy of such repurposed drugs.

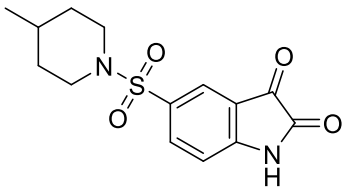
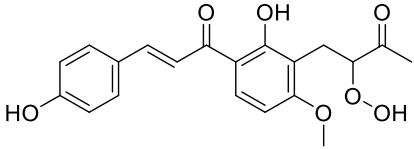
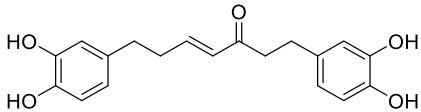
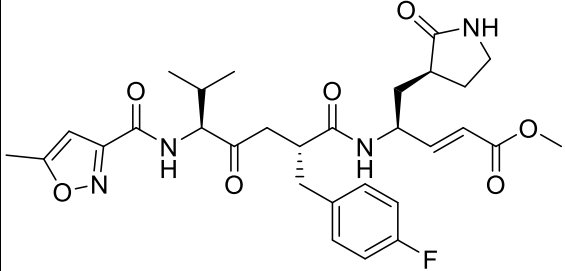
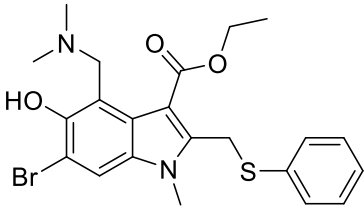
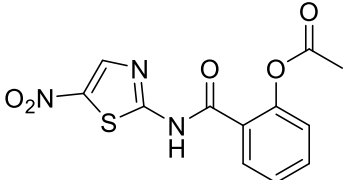
RATIONAL STUDY DESIGN. Enzymes generally have binding sites that recognize small molecules and thus, they are comparatively more druggable than non-enzymatic proteins. We have selected seven essential coronavirus enzymes as targets, namely 3CLPro, PIPro, RdRP, Helicase, NendoU, ExoN and 2O-MT, and subjected them to virtual screenings. Details of these targets are described in the next section below. The 3D structures were accessed from among the available PDB X-ray crystal structures as well as from predicted structures available from the I-Tasser server (<https://zhanglab.ccmb.med.umich.edu/COVID-19/>). The energy minimization and accompanying relaxation of crystal structures or of modeled proteins was carried out using the Protein Preparation Wizard followed by a short 20ns MD simulation (Schrödinger LLC, 2020-1). Following active site selection based on data mining and COACH predictions, we performed high-throughput virtual screening (HTVS) of compounds (n=5903) approved by worldwide any regulatory bodies including the FDA secured from the Zinc database (zinc.docking.org). The screening was performed using the Virtual Screening Wizard (Schrödinger, 2020-1) consisting of three sequential docking modes (HTVS, SP, and XP). Preliminary *in-silico* virtual screening identified ~290 potential drugs based on criteria including energy, docking parameters, ligand and binding site strain energies, and fit score. Compounds specific to each target protein were further analyzed for binding free energy perturbation by the molecular mechanics' method using Prime MM-GBSA, followed by refining the hits to the best 32 drugs. A top-scoring lead from each target group was further subjected to a molecular dynamic simulation (MDS) using the Desmond module (Schrödinger LLC, 2020-1) to validate the screening pipeline; Overall Study Design(Fig1). Table 1. illustrates drugs targeting SARS-CoV-2 specific structures, and Table 2 lists drugs targeting the host proteins.

Table 1. Repurposable drugs from global approved drug libraries with identified targets within the coronavirus family of viruses

Drug Name and Structure	Viral Targets	Role of Target Enzyme	References
Remdesivir 	RdRp (RNA-dependent RNA polymerase)	Polymerase that replicates viral genome	²⁶
Ribavirin	RdRp	Polymerase that replicates viral genome	²⁷⁻²⁹

			
<p>Favipiravir</p> 	RdRp	Polymerase that replicates viral genome	28,30
<p>Galidesivir</p> 	RdRp	Polymerase that replicates viral genome	31
<p>Aurine tricarboxylic acid</p> 	RdRp	Inhibits polymerase from replicating viral genome	27
<p>Lopinavir</p> 	3CLpro (coronavirus main protease)	Inhibits protease that cuts viral polyproteins into their functional units	32
<p>Lopinavir</p> 	PLpro (papain-like protease)	Protease that cleaves viral polyproteins into functional units	32

<p>Darunavir</p> 	3CLpro and/or PLpro	Protease that cleaves viral polyproteins into functional units	³³
<p>K777</p> 	3CLpro and/or PLpro	Protease that cleaves viral polyproteins into functional units	²⁷
<p>CAS 1851279-09, an analog of K777</p> 	3CLpro and/or PLpro	Protease that cleaves viral polyproteins into functional units	^{34,35}
<p>CAS 1851280-00-6</p> 	CLpro and/or PLpro	Protease that cleaves viral polyproteins into functional units	^{34,35}
<p>CAS 2409054-43-7</p> 	3CLpro and/or PLpro	Protease that cleaves viral polyproteins into functional units	^{34,35}

<p>CAS 452088-38-9</p> 	3CLpro and/or PLpro	Protease that cleaves viral polyproteins into functional units	^{34,35}
<p>CAS 2409054-44-8</p> 	3CLpro and/or PLpro	Protease that cleaves viral polyproteins into functional units	^{34,35}
<p>Hirsutenone</p> 	3CLpro and/or PLpro	Protease that cleaves viral polyproteins into functional units	^{34,35}
<p>Rupintrivir</p> 	3CLpro and/or PLpro	Protease that cleaves viral polyproteins into functional units	³⁶
<p>Umifenovir (Arabidol)</p> 	Spike (S) glycoprotein	Viral surface protein responsible for binding to the ACE2 host cell receptor	³⁷
<p>Nitazoxanide</p> 	Unknown	May inhibit viral protein expression	²⁸

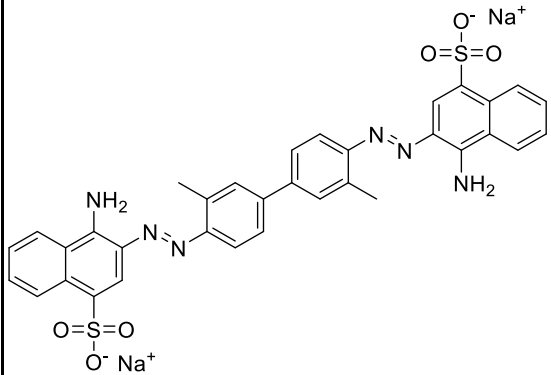
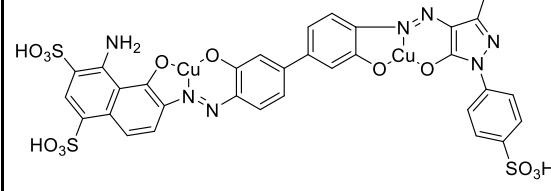
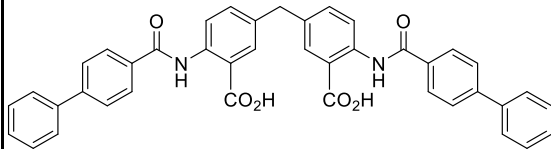
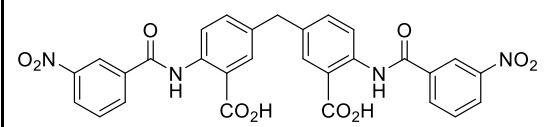
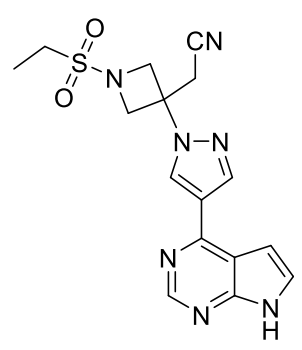
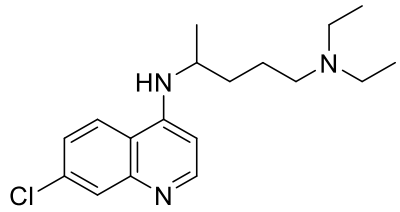
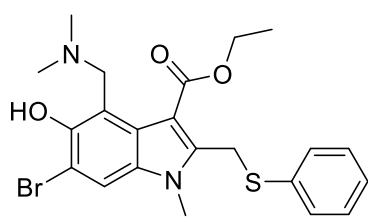
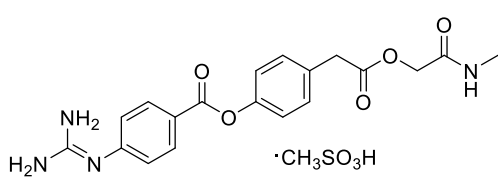
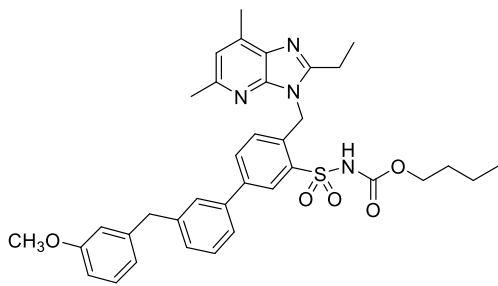
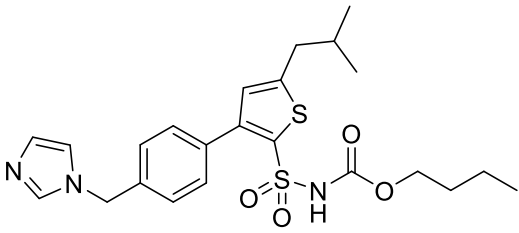
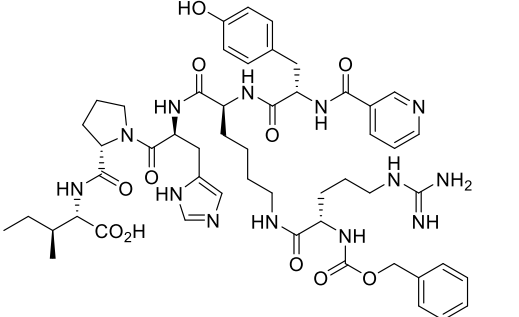
<p>Benzopurpurin B</p> 	Endoribonuclease NSP15	Nonstructural protein that plays an essential role in viral life cycle	³⁸
<p>NSC-306711</p> 	Endoribonuclease NSP15	Nonstructural protein that plays an essential role in viral life cycle	³⁸
<p>C-473872</p> 	Endoribonuclease NSP15	Nonstructural protein that plays an essential role in viral life cycle	³⁸
<p>C-467929</p> 	Endoribonuclease NSP15	Nonstructural protein that plays an essential role in viral life cycle	³⁸

Table 2. Repurposable drugs from global approved drug libraries that have known interactions with host proteins/pathways. These drugs were selected from literature showing applications against the coronavirus family.

Drug Name	Host Targets	Role of Target Protein	References
-----------	--------------	------------------------	------------

<p>Baricitinib</p> 	JAK kinase	Non-receptor tyrosine kinase that transduces cytokine-mediated signals	³⁹
<p>Chloroquine</p> 	Endosome/Angiotensin-Converting Enzyme-2 (ACE2)	Viral receptor protein on host cells which binds to viral spike protein	⁴⁰
<p>Umifenovir (Arbidol)</p> 	ACE2	Viral receptor protein on host cells which binds to viral spike protein	³⁷
<p>Camostat mesylate</p> 	TMPRSS2 (transmembrane protease, serine 2)	Protease produced by host cells that facilitates the binding of the spike protein to ACE2	⁴¹
<p>L-163491</p> 	AT2 (angiotensin AT2 receptor)	Effector involved in blood pressure and volume regulation of the cardiovascular system	⁴²

<p>C-21 (CAS 477775-14-7)</p> 	AT2	Effector involved in blood pressure and volume regulation of the cardiovascular system	42
<p>CGP-42112A</p> 	AT2	Effector involved in blood pressure and volume regulation of the cardiovascular system	42

Drug Repurposing for COVID-19: While drugs have initially been produced for use against a specific target and disease, drug repurposing offers a new and faster approach to initiate research-based methodologies. The utility of protein modeling and molecular docking has shown that approved drugs specified for certain uses can have a significant impact on other diseases⁴³. For example, loperamide is an approved drug for controlling acute and chronic diarrhea that has exhibited inhibition of the MERS-CoV replication cycle. A number of studies are currently in progress exploring the use of antiviral drugs that were approved for influenza, hepatitis C virus, and human immunodeficiency virus (HIV) 1 against COVID-19, though with limited efficacy as well as at least in some cases added morbidity due to serious side effects. When a drug is repurposed with efficacy and safety demonstrated for other diseases, the timeline to availability to the patient population is reduced, the cost of production is lower, and the distribution channels are already in place. So far, no drugs have been approved specifically for COVID-19, although several studies are underway with the goal of repurposing drugs with other indications as summarized herein.

On March 18, 2020, the WHO launched a multinational clinical trial investigating a number of drugs in clinical trials to evaluate their efficacy against COVID-19, but these trials remain inconclusive⁴⁴. One example of repurposing is the use of hydroxychloroquine (H-CQ), an antimalarial repurposed for COVID-19, that is showing mixed results, with the FDA recently (April 24th) issuing warning after drug-induced deaths. Other drugs or combinations of drugs that are or will be tested include remdesivir, combinations of lopinavir and ritonavir, and lopinavir, ritonavir and interferon beta, and chloroquine or hydroxychloroquine. These treatments regimens will be evaluated relative to appropriate controls, which in this case, refers to standard care including respiratory support as required.

Recent reports have suggested that Remdesivir may be efficacious in treating COVID-19, including a study that showed that this antiviral drug successfully inhibited MERS-CoV replication in monkey models⁴⁵. Remdesivir is a mono-phosphoramidate adenosine nucleotide analog, which is metabolized to its active form, GS-441524. This active form interferes with the functioning of viral RNA polymerase and evades proofreading by viral exoribonuclease leading to decrease in viral RNA production²⁶. Remdesivir was first showcased as a promising antiviral against Ebola when it showed successful activity against Ebola variants in cell based assays and in a rhesus monkey model³¹. Remdesivir was then taken into various clinical trials

with little to no success in comparison to other candidates that proved to be more effective⁴⁶. This raises the question whether it will again prove to be ineffective in the clinical setting, after demonstrated success in the laboratory settings, but initial results are promising. Lopinavir-Ritonavir combinations sold as Kaletra or Aluvia by AbbVie are also under evaluation for the treatment of COVID-19. Lopinavir is an HIV-1 aspartate protease inhibitor. Ritonavir is a potent inhibitor of cytochrome P450 3A4 and is combined with lopinavir to increase lopinavir's plasma half-life through diminishing its metabolism⁴⁷. On March 18, 2020, a study published in the *New England Journal of Medicine* detailed a clinical trial using lopinavir-ritonavir in adult patients with severe COVID-19⁴⁷. The study concluded that the lopinavir-ritonavir combination did not improve survival or recovery time, and instead showed severe adverse effects in patients. However, the authors noted that more severe cases of COVID-19 were enrolled in this study than in some other clinical trials. Therefore, it is prudent to wait for definitive clinical results evaluating the efficacy and safety of lopinavir-ritonavir versus COVID-19.

Lastly, chloroquine is a medication primarily used in the treatment of malaria that belongs to the 4-aminoquinoline drug class. In vitro antiviral activity of chloroquine has been known since 1969, although through the mechanism for this activity remains undetermined⁴⁸. More recent studies suggest that chloroquine may block viral infection by increasing the endosomal pH required for viral-host cell fusion, further, this drug has been shown to interfere with the glycosylation of cellular receptors⁴⁰. Chloroquine has been widely used in human patients for a variety of other indications with a fairly safe track record. The question remains whether this treatment will prove to be efficacious and safe for COVID-19 patients in a clinically robust trial, although cardiac liabilities may prove to be limiting. Beyond the drugs just mentioned, there are various other candidates in development or being tested with unknown mechanisms of action in SARS-CoV-2 specifically.

Identifying SARS-CoV-2 essential proteins as targets for repurposable drugs: Out of many proteins (~29) known to be produced by the virus, there are several critical non-structural proteins in SARS-CoV-2 that may be valuable targets for antiviral drugs. In the *coronaviridae* family, a replicase is used to translate most of the viral genomic RNA to synthesize two replicase polyproteins, pp1a and pp1ab. These two polyproteins are processed by two proteases, (1) Papain-Like Protease (PLpro) and (2), coronavirus 3-Chymotrypsin-Like Protease (3CLpro), generating 16 nonstructural proteins⁴⁹⁻⁵¹. This proteolytic processing is essential for generating functional replication complexes⁵². As such, both PLpro and 3CLpro are promising antiviral targets and have already shown promise against COVID-19 in the drug combination lopinavir-ritonavir. PLpro has a core catalytic domain containing 316 amino acids. This protease cleaves the N-terminal region of the polyprotein to generate three different nonstructural proteins (1/2/3). It is also suggested that PLpro may have de-ubiquitinating activity, due to its structural similarities with cellular de-ubiquitinating enzymes⁵³. The enzyme 3CLpro contains a cysteine-histidine dimer within its active site that directs proteolytic activity. This protease has the ability to cleave 11 different sites of the replicase polyprotein to produce a mature protein that anchors replication/transcription complexes and releases mature NSPs. Structural analyses and computational screening with 3CLpro as a target have shown promising results for drug candidates against SARS-CoV^{35,36}.

(3) Viral non-structural protein (nsp) 14: Nsp14 has been implicated in SARS-CoV-2 as possessing two different activities: an exoribonuclease (**ExoN**) activity acting on both ssRNA and dsRNA in a 3' to 5' direction, and an N7-guanine methyltransferase activity (N7-MTase)^{54,55}. The activity of N7-MTase adds the N7-methyl guanosine cap during mRNA cap synthesis that is necessary for nsp16, activated by nsp10, to facilitate 2'-O-ribose methylation of the viral mRNA cap^{56,57}. 2'-O-Methylation is critical for CoV RNA to avoid host recognition^{58,59}. 2'-O-Methylation is further discussed below. ExoN activity has been suggested to be important for CoV replication and transcription, as well as for RNA proofreading during its replication. Using human CoV 229E and CoV murine hepatitis virus (MHV) respectively, Minskaia et al. (2006) and Eckerle et al. (2007) demonstrated that ExoN active-site mutants possess defects in viral RNA synthesis^{55,60}. Eckerle et al. (2007) additionally demonstrated that ExoN active-site mutants exhibit reduced replication fidelity⁶⁰. Although there are no reports as of yet revealing drugs that successfully target guanine-N7 methyltransferase (ExoN) for treatment of SARS-CoV or MERS-CoV, given that ExoN is

important in coronaviruses for viral RNA synthesis and replication fidelity as well as for avoiding recognition of CoV RNA by the host, we feel it is a promising drug target.

(4) Nonstructural uridylyate-specific endoribonuclease (NendoU) Nsp-15 activity is found in the N-terminal domain. This active site has been shown in MERS-CoV and SARS-CoV and is suggested to be a genetic marker common to coronaviruses. MERS-CoV Nsp16 appears to display unique features compared to its homologs. Nsp7/Nsp8 display higher binding affinity for Nsp15, also affecting enzymatic activity. Nsp15 from SARS-CoV appears to be an inhibitor of mitochondrial antiviral signaling adaptor, inducing apoptosis. Nsp15 activity is stimulated by manganese ions (Mn^{2+}), and the enzymes generate 2'-3' cyclic phosphate ends⁶¹. Nsp15 functions as a homohexamer, although the enzyme has some activity as a monomer⁶². The structures of MERS-Nsp15 and SARS-Nsp15 have been superimposed showing high homology⁶³. Previous studies established that Nsp15 from both SARS-CoV and MHV can be stimulated by Mn^{2+} ⁶⁴. The activity of MERS-Nsp15 increased with the addition of Mn^{2+} , suggested by improved RNA binding affinity. The spatial arrangements revealed that residues S290 and Y339 in MERS-Nsp15 correspond to residues S293 and Y342 in SARS-Nsp15, which are postulated to interact with the substrate and confer uridylyate specificity⁶⁴, suggesting that there is conserved recognition for uridylyate.^{63,65,66}

(5) 2'-O-Methyltransferase (2'-O-MT). Following addition of the N7-methyl guanosine cap, nsp16, activated by nsp10, mediates mRNA cap 2'-O-ribose methylation to the 5'-cap structure of viral mRNAs. This has been shown in SARS-CoV and MERS-CoV, and suggested to be universal to coronaviruses^{67,68}. 2'-O-Methylation is important for the host immune system to discern self RNA from non-self RNA. Thus, through 2'-O-methylation of viral RNA, coronaviruses can subvert host innate immune responses by avoiding host recognition of their RNA⁶⁸. Menachery et al. (2014) demonstrated the requirement of 2'-O-methyltransferase (2'-O-MT) activity for SARS-CoV pathogenesis by showing that without 2'-O-methyltransferase (2'-O-MT), there is significant reduction of SARS-CoV both *in vitro* and *in vivo*. This was indicated by reduced viral titers and viral replication, as well as less weight loss and reduced breathing dysfunction in mice⁶⁸. Similarly, the importance of nsp16, and thus the activity of 2'-O-methyltransferase (2'-O-MT), has also been shown for MERS-CoV pathogenesis. Menachery et al. (2017) introduced mutations in the MERS-CoV NSP16 conserved KDKE motif, which resulted in significant attenuation of viral load relative to the controls both *in vitro* and *in vivo*⁶⁷. Despite there being no publications to date detailing drugs that target 2'-O-methyltransferase to treat SARS-CoV or MERS-CoV, we are interested in 2'-O-MT as a potential drug target because of its role in avoiding recognition of CoV RNA by the host and its importance for SARS-CoV and MERS-CoV pathogenesis.

(6) Viral helicase is essential to viral genome replication and is therefore a potential target for antiviral drug development. Virus-encoded RNA helicases have important roles during viral life cycles for folding and replication of viral RNA⁶⁹. As such, Nsp13 possesses NTPase and RNA helicases to facilitate hydrolysis of NTPs and unwind RNA. In one study, it was demonstrated that myricetin and scutellarein are strong inhibitors of SARS-CoV helicase protein by affecting its ATPase activity⁷⁰. Helicase is a multi-functional protein with a zinc-binding domain in the N-terminus displaying RNA and DNA duplex-unwinding activities with 5' to 3' polarity. Activity of helicase is dependent on magnesium. As such, bismuth salts have been shown to inhibit NTPase and RNA helicase activities of SARS-CoV-2 nsp13⁷¹ (<https://zhanglab.ccmb.med.umich.edu/C-I-TASSER/2019-nCov/>). Sequence annotation by Ivanov et al.⁶¹ has shown that SARS-CoV nsp13 is divided into three domains: (i) an N-terminal Zn(II) binding domain and (ii) a hinge domain and (iii) a helicase domain⁶⁹. Little is known of the viral non-structural protein (nsps) 12 activity, but activity occurs on two domains, on the N-terminal subunit NiRAN, and on the C-terminus. These sites have been shown in SARs-CoV and are suggested to be applicable to coronaviruses.^{72,73}

(7) RNA-directed RNA polymerase (RdRp) plays a critical RNA replication in RNA viruses due to its function of catalyzing template synthesis of polynucleotides in the 5'-3' direction. Further, RdRp is an essential for initiation RNA replication in the host cell, a key step in the RNA viruses infection cycle^{74,75}. Jingyue Ju et al. (2020) have demonstrated the importance of RdRp activity for SARs-CoV pathogenesis. They showed that without RdRp, there is a complete disruption of SARs-CoV -RNA replication and viral growth halted. More than this, Jingyue Ju et al. (2020) suggested that the hepatitis C drug EPCLUSA

(Sofosbuvir/Velpatasir) would target the active site of RdRp to inhibit coronaviruses⁷⁶. RdRp is an established drug target for the treatment of SARS-CoV due to its role in viral RNA replication and its importance for SARS-CoV pathogenesis. We are particularly interested in targeting RdRp since it has been suggested to be targeted by hepatitis C drug EPCLUSA (Sofosbuvir/Velpatasir) for inhibition of coronaviruses.

METHODS

Protein(Receptor) structures. The crystal structures of NSP3 (PDB ID- 6W02), NSP9(PDB ID- 6W4B), NSP15 (PDB ID- 6VWW) from SARS CoV-2 were obtained from Protein Data Bank [<http://www.rcsb.org/pdb/home/home.do>]. The crystal structures of COVID-19 main protease (NSP5) in complex with Z44592329 (ID:5r83) were obtained from the Protein Structure Database of Europe (<https://www.ebi.ac.uk/pdbe>). QHD43415(<https://zhanglab.ccmb.med.umich.edu/C-I-TASSER/2019-nCov/>): the I-TASSER models were obtained for NSP3(QHD43415_3), NSP5 (QHD43415_5), NSP11(QHD43415_11), NSP12 (QHD43415_12), NSP13(QHD43415_13), and NSP14 (QHD43415_14)⁷⁷.

Target Proteins(Receptors) preparation. Protein preparation was performed using the Protein Preparation Wizard in Maestro (Schrödinger, L. L. C. "Schrödinger Release 2020-1." (2020).). All co-crystallized atoms including calcium and chlorine were deleted. Crystal ligands were not deleted because they were used for grid generation. Each of the seven models developed were optimized and then minimized using the OPLS3e force field (Schrödinger- LLC 2020-1." (2020). Further the models were subjected to a 20 ns MD simulation (MDS). The target complex with *trans*-isomers was subjected to MDS and trajectory analysis was conducted using the Desmond software (Schrödinger-LLC 2020-1). The full system was prepared by using Maestro's Protein Preparation Wizard. The system was solvated in TIP3P water models with 0.15 M NaCl and placed in physiological solution. A simulation box covering the entire enzyme system was introduced with a 10 Å buffer space. The simulation was run for 20 ns at 300 K and standard pressure (1.01325 bar). OPLS-AA 2005 force field parameters were elected for utilization during this preparation and all later simulations.

Target library preparation. A virtual library of n=5903 drug compounds was downloaded from the Zinc database (<http://zinc.docking.org/substances>) under the 'world' subset (approved drugs in major jurisdictions, including the FDA, i.e DrugBank approved). The database was then checked for redundancy, and duplicates were removed. Ligand preparation was performed using LigPrep, which generated variations of the ligands, eliminated reactive species and optimized the ligands. Optimization was performed under the OPLS3e force field. EPIK minimization was performed on possible states at pH 7.0 ± 2.0. Tautomers were generated for each ligand retaining specific chirality combinations with a maximum of 32 structures per ligand (Schrödinger, L. L. C. 2020-1).

Receptor grid generation. COACH analysis was performed to determine the location and size of the active site⁷⁸. The shape and properties of the receptor are represented on a grid to ensure that possible active compounds are not missed. The centroid of the COACH predicted binding pocket residues and was used to generate grids using default values of protein atom scaling (1.0 Å) within a cubic box. The force field employed for grid generation was OPLS3e⁷⁹.

High-Throughput Virtual Screening (HTVS). The screening was performed with default parameters including ionization states, Epik state penalties within the Glide (Grid-based ligand docking from energetics) module of Schrödinger suite⁸⁰. The scaling factor was maintained at a default of 0.8 and a partial charge cut-off was limited to 0.15. The OPLS3e force field was used during the docking process. The HTVS ligand docking was the first to be performed, followed by SP and XP docking on the top 10%

of scoring hits from each previous step. The XP docking aids in removing false positives, and the scoring function is much stricter than the HTVS. The greater the XP Glide score, the better calculated affinity of the hit in binding to the protein target. Further, the estimation of free binding energies for the best hit-docked complexes using MM force fields and implicit solvation was performed using the molecular mechanics/generalized Born surface area (MM-GBSA) method within virtual screening workflow of Schrödinger suite 2020-1. The binding energy was calculated based on the following equation.

$$\Delta G = E_{\text{complex}}(\text{minimized}) - (E_{\text{ligand}}(\text{minimized}) + E_{\text{receptor}}(\text{minimized}))$$

The leads were ranked on the basis of binding free energy calculation for their respective protein-ligand complexes.

Molecular Dynamics Simulation (MDS). The top hit for each target was subjected to a 20 ns MD simulation (100 ns for XAV-939 + 3CLPro) as described above in the Target/receptor Preparation section to validate the interaction and thereby the HTVS pipeline performance.

RESULTS AND DISCUSSION

Following *in-silico* HTVS, molecular modeling, MDS, and utilizing resources from the literature, we identified a series of potential leads molecules from the repurposable drug libraries against specific proteins that are critical for the ability of SARS-CoV-2 to infect and reproduce within the host cell. Additionally, all of the simulated hit-target complexes were found to be strongly interacting and exhibited highly stable binding indicating the potential of being used for treating COVID-19. Outputs from these analyses are presented in tables and graphically, and are discussed in the following sections.

Doc k ID	Drug Name	Indicated target	Glide Energy	DockScore	LipophilicEvdW	HBond	Electro	ExposPenal	RotPenal
A	Maltotetraose	Substances that inhibit the growth or reproduction of BACTERIA	-58.44	-11.31	-1.54	-6.96	-2	0.09	0.1
B	Natural Crocin and/or Crocetin	for treating neurodegenerative disorders of the central nervous system, e.g. nootropic agents, cognition enhancers, drugs for treating Alzheimer's disease or other forms of dementia	-53.89	-10.36	-1.68	-6.05	-1.84	0.14	0.07
C	Paclitaxel	inhibits the disassembly of microtubules	-70.51	-8.7	-1.24	-5.03	-2	0.38	0.17
D	NADH dianion	Dianion of NADH arising from deprotonation of the two diphosphate OH groups; major species at pH 7.3.	-61.72	-8.55	-1.56	-5.69	-2	0.74	0.14
E	Iohexol	MRI contrasting agent/ histone acetyltransferase KAT2A (human)	-67.38	-6.04	-2.87	-2.84	-1.37	0.8	0.19
F	Heparin	Anticoagulant	-86.41	-12	-4.02	-12	4.02	1.1	0.07

2'-O-Methyltransferase (2'-O-MT) hits. *Maltotetraose* is an oligosaccharide of four units of alpha-D-glucopyranose linked by alpha-(1-4) bonds. This is a sugar variant of a substance that is found to inhibit the growth and reproduction of bacteria^{81,82}. *Crocin/Crocetin* are the major bioactive ingredients of saffron. There have been several studies that have shown the various efficacies of these drugs, including as neurotropic and chemotherapeutic agents^{83,84}. Crocin/Crocetin are popular agents to be tested in clinical settings due to their anti-oxidative properties⁸⁵. *Paclitaxel* is a diterpene alkaloid natural product and belongs to a family of drugs that target tubulin leading to an abnormality of the mitotic spindle assembly, chromosome segregation, and consequently defects of cell division⁸⁶. Paclitaxel is one of the most widely used anticancer drugs for the treatment of various cancers⁸⁷. Other studies have shown that low doses of paclitaxel show promise in treating some non-cancer diseases including renal and hepatic fibrosis and artery restenosis⁸⁸⁻⁹⁰. *NADH dianion* is a species of NADH that arises from the deprotonation of the two diphosphate OH groups. *Iohexol* is a compound most well-known as a nonionic, water-soluble radiographic contrast medium used especially for renal disease determination. This compound is absorbed from cerebrospinal fluid into the bloodstream and is eliminated by renal excretion. Heparin is a very interesting hit as it has been reported in multiple studies to increase the likelihood of survival of terminal COVID-19 patients^{91,92}. By mechanism that is not well understood but involves heparin's activity of reducing hypoxia as well via inhibiting the cytokine storm⁹³. There is a minor report suggesting that hepcidin hormone mimics the spike protein of Covid-19,⁹⁴ and heparin is known to interfere with hepcidin⁹⁵. This suggests that heparin's anti-COVID activity may present a multifaceted therapy option. MMGBSA re-ranking brought this molecule to the bottom despite a high glide energy score due to penalties exacted due to extra-active site exposure of the bulky compound.

Doc k ID	Drug Name	Normal target	Glide Energy	DockScore	LipophilicEvdW	HBond	Electro	ExposPenal	RotPenal
A	Lactulose	Laxative & portal-systemic encephalopathy (PSE)	-67.99	-15.22	-11.26		0.54		0.06
B	Framycetin/Paromomycin	16S ribosomal RNA	-66.49	-14.87	-6.87		0.1		0.11
C	Amikacin/Arbekacin	16S ribosomal RNA	-73.4	-14.06	-10.24		0		0.06

D	Bekanamycin	Not Available	-63.88	-14.69	-6.6	0.12			0.11
E	Lividomycin A	Not Available	-64.68	-14.6	-6.56	0.02			0.11
F	Lapatinib Ditosylate	Blocks phosphorylation of the epidermal growth factor receptor (EGFR), ErbB2, and the Erk-1 and-2 and AKT kinases; it also inhibits cyclin D protein levels in human tumor cell lines and xenografts.	-51.39	-11.15	-2.14	-5.48	-2	0.22	0.11

RNA-directed RNA polymerase (RdRp) hits. The COVID-19 RdRP is predicted to bind tightly to aminoglycosides. Drug screening reveals many hits from this class of antibiotics including Framycetin, Paromomycin, Amikacin, Arbekacin, Bekanamycin, & Lividomycin A. While aminoglycosides have a binding affinity for RNA and have been reported to inhibit binding of RdRP to the decoding loop in case of influenza⁹⁶ the complementary RNA binding site of RdRP has also been reported to be susceptible to aminoglycosides eg. neomycin B which targets HCV RdRP⁹⁷. Interestingly, the highest scoring among the aminoglycoside hits is *Paromomycin* which is an antiparasitic used to treat amoebiasis, visceral leishmaniasis and cryptosporidiosis in immunocompromised patients. With a potential to treat pulmonary tuberculosis as well, the range of indications of this drug is indeed very wide and if found effective against COVID-19, it could prove to be a valuable addition to the arsenal of combination therapies.

Lactulose is a synthetic disaccharide of galactose and fructose which can be produced by the isomerization of lactose. This compound has been used for treating bacterial infections, constipation, and cancer. An important note on lactulose is that it is not hydrolyzed by mammalian enzymes, therefore, ingested lactulose passes through the stomach and small intestine without degradation⁹⁸. *Framycetin* is an aminoglycoside antibiotic isolated from *Streptomyces lavendulae* that shows broad-spectrum antibacterial activity. This drug has been used as a therapeutic against a variety of cancers^{99,100}. *Amikacin* is an aminoglycoside antibiotic that is on the WHO list of essential medicines. It is a prokaryotic translation inhibitor that binds to the 16S ribosomal subunit. *Bekanamycin* is another aminoglycoside that inhibits prokaryotic translation by binding to the highly conserved A site of 16S rRNA in the 30S ribosomal subunit. This compound has the lowest antibacterial activity of the aminoglycosides in clinical use and manifests a moderate level of toxicity, therefore, it is no longer used as a first line antibiotic¹⁰¹. *Lividomycin A* is an aminoglycoside that shows antibiotic activity against several Gram +/- bacteria by inhibiting protein synthesis¹⁰². *Lapatinib ditosylate* is the salt of Lapatinib, a synthetic quinazoline that blocks the phosphorylation of various epidermal growth factor receptors and inhibits cyclin D protein levels in human tumor xenografts and cell lines^{103,104}.

Table.5:- Uridylate-specific endoribonuclease (NendoU) Hits									
Doc k ID	Drug Name	Normal target	Glide Energy	DockScore	LipophilicEvdW	HBond	Electro	ExposPenal	RotPenal
A	Daidzin	Aldehyde dehydrogenase, mitochondrial (human)	-68.65	-14.56	-1.9	-6.32	-2	0.05	0.11

Ba	SCHEMBL24383, ZINC8143723	Active principle of <i>Strychnos potatorum</i> Linn. Seed extracts. Known antiallergic, antianaphylactic and mast cell stabilization activity	-72.09	-14.52	-1.87	-6.28	-2	0.03	0.11
Bb	Metrizamide	Resorbable, non-ionic contrast medium.	-71.41	-14.26	-1.78	-6.32	-2	0.23	0.11
C	Haloperidol Glucuronide	Anti-depressant	-71.81	-13.48	-2.61	-9.12	-2	0.19	0.06
D	4-Hydroxyphenytoin glucuronide	Phenytoin metabolite by liver UDP-glucuronosyltransferase.	-74.49	-13.5	-1.87	-7	-2	0.18	0.19
E	acetaminophen O-β-D-glucosiduronate	A β-D-glucosiduronate that is the conjugate base of acetaminophen O-β-D-glucosiduronic acid	-70.28	-14.07	-1.51	-6.27	-2	0.1	0.11
F	p-Aminophenyl-alpha-D-Galactopyranoside	Heat-labile enterotoxin B chain	-71.44	-14.06	-1.87	-5.82	-2	0.02	0.11

Uridylate-specific endoribonuclease (NendoU) Hits. Daidzin is an isoflavone natural product found in several *Legumimosae* such as the Japanese Kudzu root and is the 7-*O*-glucoside of the isoflavone daidzein. It is shown to have anticancer and antiallergenic activities¹⁰⁵. Diadzin and Haloperidol have been identified in multiple virtual screenings^{106,107}. SCHEMBL24383 (Active principle of *Strychnos potatorum* Linn. Seed extract) has been extensively used to combat respiratory diseases such as asthma, chronic obstructive pulmonary disease (COPD) and bronchitis. Interestingly, given its predicted anti-Covid-19 activity, it may result in a dual therapeutic potential drug. Metrizamide is a non-ionic iodine-based radiocontrast agent that is widely used in lumbar myelography. It is only found in individuals that have taken this compound¹⁰⁸. Haloperidol glucuronide is a metabolite of the commonly prescribed antipsychotic drug on the WHO's list of Essential Medicines. Haloperidol is used in the treatment of schizophrenia, mania in bipolar, delirium, and other neurological diseases^{109,110} and is on the WHO's List of Essential Medicines. 4-Hydroxy phenytoin glucuronide is a metabolite of the widely used antiepileptic phenytoin. The adverse effects of phenytoin can range from moderate diseases like gingival hyperplasia to severe more effects including toxic epidermal necrolysis and teratogenic effects¹¹¹. Similarly, acetaminophen O-β-D-glucose iduronate is a metabolite of acetaminophen generated in the liver by UDP-glucuronyltransferase. It is highly water soluble and is excreted through the kidneys. Acetaminophen was recommended by WHO in the case of COVID-19 due to a concern over ibuprofen being an ACE2 inhibitor that might increase viral entry¹¹². The advisory was subsequently revised to state that both medications are appropriate¹¹³. A metabolite of acetaminophen could prove to be an added advantage of already being used as a drug. p-Aminophenyl-alpha-D-galactopyranoside is an experimental phenolic glycoside that competitively binds to heat-labile enterotoxin B pentamers by mimicking host cell receptors (intracellular adenylyl cyclase)¹¹⁴.

Table.6:- Guanine-N7 methyltransferase (ExoN) Hits									
Doc k ID	Drug Name	Normal target	Glide Energy	DockScore	Lipophilic EvdW	HBond	Electro	ExposPenal	RotPenal
A	Diosmin	Dosmin, a flavone that can be found in the plant <i>Teucrium gnaphalodes</i> . Is an agonist at the human aryl hydrocarbon receptor	-68.66	-13.26	-1.66	-6.01	-2	0.11	0.11
B	Hidrosmin	Capillary stabilizing agent	-71.34	-13.24	-2.01	-5.57	-2	0.05	0.11

C	N-Desmethyl-4-hydroxy tamoxifen beta-D-glucuronide (E/Z Mixture)	N/A	-72.69	-13.23	-1.77	-6.22	-2	0.48	0.11
D	Octane-1,3,5,7-tetracarboxylic acid	Carboxypeptidase A1	-68.77	-13.17	-1.65	-6.08	-2	0.28	0.11
E	Bempedoic acid	Metabolic activation affords ETC-1002-CoA, the pharmacologically active metabolite. ATP lyase (a.k.a. ATP synthase) plays an important part of cholesterol synthesis	-71.39	-13.15	-2.14	-5.48	-2	0.22	0.08

Guanine-N7 methyltransferase (ExoN) Hits. *Diosmin* is a flavone glycoside that is mostly found in citrus fruits. It is a non-prescribed dietary supplement that is primarily used for venous diseases, though there is limited clinical data to support its efficacy. Common adverse effects include mild gastrointestinal disturbances and cardiac arrhythmias¹¹⁵. Interestingly other studies have reported diosmin to be a coronavirus main protease inhibitor. *Hidrosmin* is a synthetic bioflavonoid that is used to treat chronic venous insufficiency of the lower limbs¹¹⁶. A crude preparation of Diosmin and Hidrosmin has been determined to be highly effective against Covid-19¹¹⁷. N-Desmethyl-4-hydroxy tamoxifen beta-D-glucuronide (E/Z Mixture) has also been identified a strongly binding ligand. *Tamoxifen* has also been proposed as an anti-COVID19 drug as it can induce autophagy associated with the unfolded protein response to kill infected cells and thus contain the virus¹¹⁸. Octane-1,3,5,7-tetracarboxylic acid B belongs to the class of organic compounds known as tetracarboxylic acids and derivatives classified under zinc ion binding compounds that target Carboxypeptidase A1.

Bempedoic acid is a prodrug that is converted to its active form in the liver. It is an FDA approved treatment for hyper cholesterolemia and has few adverse effects. This compound inhibits adenosine triphosphate citrate lyase, an enzyme within the cholesterol biosynthesis pathway¹¹⁹.

Table.7:- Helicase (hel) Hits									
Doc k ID	Drug Name	Normal target	Glide Energy	DockS core	LipophilicE vdW	HBond	Electro	ExposPenal	RotPenal
A	Inosine	Neurorestorative, anti-inflammatory, immunomodulatory and cardioprotective effects.	-72.87	-13.05	-1.76	-6.23	-2	0.66	0.11
B	5-F-UMP	Bacterial Thymidylate synthase	-57.22	-12.94	-1.79	-6.68	-2	0.13	0.08
C	Fenoterol	Agonist to Beta-2 adrenergic receptor	-57.22	-12.94	-1.79	-6.68	-2	0.13	0.08
D	Didanosine	Anti-HIV	-72.87	-12.94	-1.76	-6.12	-2	0.66	0.11
E	Doxifluridine	Not Available/Anti-cancer	-68.72	-12.9	-1.88	-5.81	-2	0.09	0.13

Helicase (hel) Hits. The FDA approved drug ivermectin recently showed significant anti-COVID-19 antiviral activity, suggesting its therapeutic potential¹²⁰. While the target of ivermectin in COVID-19 is yet to be confirmed, it has been reported that its antiviral activity in the case of flaviviruses, particularly Australian Kunjin virus (West Nile virus variant)¹²¹ is based on targeting viral helicases. While our screening did not show ivermectin as a top helicase inhibitor, its binding activity established viral helicase as an important target in COVID-19. We found several small molecule compounds including inosine, 5-F-UMP, fenoterol, didanosine and doxifluridine as potential helicase inhibitors. While *Inosine*, *5-F-UMP* and *Fenoterol* have high affinity towards ATP-Nucleic acid interface, our top target against Helicase is *inosine*. Inosine is nucleoside commonly found in tRNAs and is essential for proper translation of the genetic code in wobble base pairs. It has been tried in various clinical settings, most notably in multiple sclerosis¹²². *5-*

F-UMP is a pyrimidine ribonucleoside 5'-monophosphate having 5-fluorouracil as the pyrimidine component. It shows antineoplastic activity by being incorporated in RNA and it inhibits RNA processing, thereby inhibiting cell growth. *Fenoterol* is a β adrenoreceptor agonist that is used as an inhaled bronchodilator asthma medication¹²³. *Didanosine* is particularly interesting as it is a reverse transcriptase (HIV) inhibitor¹²⁴. Also, Didanosine has been profiled as a beneficial drug in the case of the COVID-19 type of lung fibrosis by matching single cell RNA sequencing data¹²⁵. Inhibition of inosine-5'-monophosphate dehydrogenase (IMPDH) has been shown to control COVID-19 replication¹²⁶, which could be due to inosine accumulation. *Didanosine* is also a medication used to slow the progress of HIV/AIDS and is a nucleoside analogue of adenosine. There are several common adverse effects associated with this medication including diarrhea, vomiting, and peripheral neuropathy¹²⁷. *Fenoterol* has already been recommended to reduce severe pulmonary symptoms of COVID-19 patients¹²⁸. *Doxifluridine* has been suggested as a possible COVID-19 inhibitor based on similarities with active antivirals already tested by artificial intelligence¹²⁹. *Doxifluridine* is a nucleoside analog prodrug that interferes with RNA transcription by competing with uridine triphosphate for incorporation into the RNA strand. It is used as a cytostatic agent in chemotherapy in several countries in Asia¹³⁰.

Doc k ID	Drug Name	Normal target	Glide Energy	DockScore	LipophilicEvdW	HBond	Electro	ExposPenal	RotPenal
A	Troloxerutin	Not known	-73.57	-13.5	-1.62	-2	-7.17	0.19	0.09
B	4-O-(4,6-Dideoxy-4-[[4,5,6-trihydroxy-3-(hydroxymethyl)cyclohex-2-en-1-yl]amino]-beta-D-lyxo-hexopyranosyl)-alpha-D-erythro-hexopyranose	Pancreatic alpha-amylase (DB03495)	-61.8	-13.79	-1.53	-2	-5.92	0.05	0.11
C	4,6-Dideoxy-4-[[4,5,6-trihydroxy-3-(hydroxymethyl)cyclohex-2-en-1-yl]amino]-alpha-D-lyxo-hexopyranosyl-(1->4)-alpha-D-threo-hexopyranosyl-(1->6)-alpha-L-threo-hexopyranose	Pancreatic alpha-amylase (DB02889)	-75.87	-13.3	-1.72	-2	-5.36	0.25	0.11
D	Hyaluronic acid	Supplement	-64.36	-13.24	-2.04	-2	-5.21	0.4	0.11
E	Monoxerutin	Not known	-64.68	-14.6	-13.92	-2	-6.56	0.02	0.11
F	Anastrozole	Non-steroidal aromatase inhibitor (AI)							

Papain-like proteinase (PIPro)Hits. *Troloxerutin* is a naturally occurring flavonoid that has been reported to show promise as a vasoprotective agent by improving hepatic homeostasis¹³¹. As there have been many *in silico* drug screening efforts with the coronavirus Main Protease that include troloxerutin as a potential inhibitor of 3CLPro¹³². Also, the famous 'Chai-Ling decoction' a Chinese medicine herbal formulation with reported protection from SARS, MERS and now COVID-19 has troloxerutin as a major component^{133,134}. The identified hit 4-O-(4,6-Dideoxy-4-[[4,5,6-trihydroxy-3-(hydroxymethyl)cyclohex-2-en-1-yl]amino]-beta-D-lyxo-hexopyranosyl)-alpha-D-erythro-hexopyranose is an aminocyclitol glycoside, as well as as 4,6-dideoxy-4-[[4,5,6-trihydroxy-3-(hydroxymethyl)cyclohex-2-en-1-yl]amino]-Aapha-D-lyxo-hexopyranosyl-(1->4)-alpha-D-threo-hexopyranosyl-(1->6)-alpha-L-threo-hexopyranose have been shown to target pancreatic alpha-amylase¹³⁵. Both of these compounds belong to the class of aminocyclitol glycosides similar to streptomycin. This class of compounds have been used previously to target RNA metabolism of viruses¹³⁶. *Hyaluronic acid* is a non-sulphated glycosaminoglycan (GAG) and is composed of repeating polymeric disaccharides of D-glucuronic acid and N-acetyl-D-glucosamine linked by a glucuronidic β (1 \rightarrow 3) bond¹³⁷. It is a key molecule involved in skin moisture that has the capability to retain water. *Monoxerutin* is another flavonoid which has been patented to be used against Hepatitis C¹³⁸. *Anastrozole* is an aromatase inhibitor approved by the FDA to treat postmenopausal women diagnosed with

advanced stage hormone receptor positive breast cancer and hormone receptor positive early stage breast cancer after surgery^{139,140}.

Dock ID	Drug Name	Normal target	Glide Energy	DockScore	LipophilicEvdW	HBond	Electro	ExposPenal	RotPenal
A	XAV-939	Not known; Anti-cancer	-71.17	-12.66	-5.74	-5.98	-1.46	0.37	0.15
B	Crocin	Arthritis	-63.96	-11.56	-3.24	-6.68	-2	0.23	0.14
C	Iopromide	non-ionic X-ray contrast agent	-77.95	-11.07	-5.34	-4.64	-1.63	0.39	0.15
D	Troloxerutin	Chronic Venous Insufficiency	-64.53	-10.69	-4.69	-4.29	-1.42	0	0.11
E	Isoquercetin	Anti-cancer	-73.56	-10.31	-4.89	-4.42	-1.71	0.54	0.17
F	Danoprevir	Inhibitor of the HCV NS3/4A protease	-66.83	-10.03	-4.73	-4.01	-1.44	0.04	0.11
G	Cefoperazone	Cephalosporin; antibacterial	-79.52	-7.8	-3.14	-4.22	-1.67	0.7	0.19
H	Nevirapine	Non-nucleoside reverse transcriptase inhibitor (NNRTI)	-63.17	-7.79	-3.31	-3.25	-1.09	0.11	0.14
I	Pentostatin	Adenosine deaminase; anti-cancer	-81.01	-7.12	-3.78	-3.74	-2	2.09	0.19
J	Cladribine	Synthetic purine nucleoside that acts as an antineoplastic agent	-78.93	-6.86	-5.19	-1.48	-1.09	0.85	0.19

Main proteinase (3CIPPro) Hits. *XAV-939* is a beta-catenin signaling inhibitor that has been shown to have promise in treating prostate cancer¹⁴¹. *XAV-939* is also an effective inhibitor of PARP and Wnt pathway. PARPs enhance IFN γ production and can halt viral infections^{142,143}. Thus, a dual mode of action is expected of *XAV-939* if it is found to inhibit the main protease as well. *Crocin* is carotenoid diester that is responsible for the color of saffron, and is popularly used in India as a treatment for arthritis and psychological disorders¹⁴⁴. *Loperamide* is used to treat gastrointestinal symptoms including diarrhea with few side effects and is on the WHO's List of Essential Medicines. *Isoquercetin* is a flavonoid natural product that can be isolated from various plant species and has shown promise as an anti-cancer agent¹⁴⁵. *Danoprevir* is a 15-membered ring macrocyclic peptidomimetic inhibitor of the hepatitis C protease NS3/4A¹⁴⁶. Other virtual drug screenings have reported danoprevir as a possible coronavirus main protease inhibitor¹⁴⁷. In clinical trials, danoprevir had a positive effect on recovery and faster discharge of COVID-19 patients¹⁴⁸. *Cefoperazone* is a cephalosporin antibiotic. It is one of the few cephalosporin antibiotics effective in treating *Pseudomonas* bacterial infections¹⁴⁹. In China most of the treatment regimens reported using cefoperazone to prevent secondary infections in COVID-19 patients^{150,151}. *Nevirapine* is a non-nucleoside reverse-transcriptase inhibitor¹⁵². This compound is FDA approved for use in adult patients infected with HIV-1. Nevirapine has also been revealed in various *in-silico* drug screening with the main protease^{153,154}. *Pentostatin* is a purine analog that is widely used as a treatment for hairy cell leukemia¹⁵⁵. Similar to pentostatin, *cladribine* is also a therapy for hairy cell leukemia. And also like nevirapine, cladribine has also been predicted to block main protease 3CLPro in many reports^{154,156}.

Approved drugs encompass major jurisdictions including the FDA approved drugs (i.e. DrugBank). Virtual screening was performed to investigate which compounds are predicted to have a strong binding affinity to key COVID-19 proteins. With proteins identified as potential targets for the World approved drugs/compound library, our study demonstrated that, in principle that multiple repurposable drugs should be used to treat COVID-19 as targeted therapies. The identified drug molecules have been further summarized to better represent their properties where possible including dose, toxicity, pharmacodynamic data and combinatorial compatibility. These properties will assist clinicians in making a decision on whether they are suitable to test in treating COVID-19 patients and also help to determine if they are suitable for multi-drug therapy (MDT) regimen.

Table 10. Description of virtual screening hits for reproducibility; general toxicity, pharmacodynamics, approved dosage and drug-drug interaction for combination therapy.

Drug	Current Indication	Toxicity	Pharmacodynamics	Approved Dose	drug-drug interactions
Paclitaxel	Treat various cancers	Bone marrow suspension, peripheral nervous system neurotoxicity, mucositis.	Antimicrotubule agent. Stabilizes microtubules by preventing depolymerization. Results in inhibition of mitosis and interphase.	Injection - 100mg/16.7mL	Danoprevir - Metabolism of Paclitaxel slows down. Anastrozole- Metabolism of Paclitaxel slows down. Heparin- Risk of severe bleeding can be increased. Didanosine- Increase Neurotoxic activities. Haloperidol- Metabolism of Paclitaxel slows down. Doxifluridine- the risk of adverse effects can increase when Paclitaxel is combined. Chloroquine- Metabolism of Paclitaxel can slow down. Phenytoin- Serum Concentration of Paclitaxel can be decreased. Hydroxychloroquine- the risk of adverse effects can increase when Paclitaxel is combined.
Danoprevir	Hepatitis C treatment	No Data Available	No Data Available	No Data Available	Paclitaxel-Metabolism of Paclitaxel slows down.
Anastrozole	Treat breast cancers in postmenopausal women	Incomplete signs of toxicity as listed on Drugbank.	Prevents the conversion of testosterone to estrogen to suppress cancer growth.	Oral- 1 mg/1	Paclitaxel-The metabolism of Paclitaxel can be decreased Chloroquine-Metabolism decreases when combined with Anastrozole. Phenytoin-Metabolism decreases when combined with Anastrozole.
Heparin	Anticoagulant	Heparin induced thrombocytopenia, osteoporosis and spontaneous vertebral fractures.	Inhibits reactions that lead to coagulation/clotting of blood.	Intravenous - 100 [USP'U]/1mL	Paclitaxel-The risk or severity of bleeding can be increased Phenytoin-The Therapeutic efficacy of Heparin can be increased.
Didanosine	HIV treatment	Pancreatitis, peripheral neuropathy, diarrhea, hyperuricemia, and hepatic dysfunction	Acts as a chain terminator of DNA synthesis. Inhibits HIV reverse transcriptase.	Oral - 400 mg/1	Paclitaxel-Didanosine may increase the neurotoxic activities of Paclitaxel Haloperidol-Can decrease the excretion rate of Didanosine, thus resulting in higher serum levels. Chloroquine- Can decrease the excretion rate of Didanosine, thus resulting in higher serum levels.
Vidarabine	Treatment of herpes, poxviruses, rhabdoviruses, etc.	No toxicity reported	Stops the DNA replication of herpes. Prevents the formation of phosphodiester bridges between bases.	Topical- 30mg/1g	No Data Available

Haloperidol	Antipsychotic	Acute oral toxicity	Effective for positive symptoms of schizophrenia. Blocks dopaminergic, cholinergic, and histaminergic receptors.	100 mg/1g (multiple dosages - intramuscular)	Didanosine- Haloperidol Can decrease the excretion rate of Didanosine , resulting in higher serum levels. Chloroquine- Metabolism of Chloroquine slows down when combined with Haloperidol. Phenytoin- Metabolism of Haloperidol decreases when combined with Phenytoin. Hydroxychloroquine- Metabolism of Haloperidol decreases when combined with Hydroxychloroquine.
Doxifluridine	Gastric cancer	No Data Available	No Data Available	No Data Available	Paclitaxel-The risk or severity of adverse effects can be increased Phenytoin- Serum concentration increases when combined with Doxifluridine. Hydroxychloroquine- The risk or severity of adverse effects can increase
Daidzin	Antidipsotropic	No Data Available	No Data Available	No Data Available	No Data Available
Diosmin		No Data Available	No Data Available	No Data Available	No Data Available
Chloroquine	Anti-malarial to treat and prevent malaria	Headache, drowsiness, visual disturbances, nausea, vomiting. Overdose can include: cardiac arrest, respiratory arrest.	Inhibits the action of heme polymerase which causes the buildup of toxic heme in Plasmodium species.	Oral - 250 mg	Paclitaxel-The metabolism of Paclitaxel can be decreased Anastrozole- Metabolism of Anastrozole can be decreased when combined with Chloroquine. Didanosine- Chloroquine decreases the excretion rate of Didanosine, increasing serum level. Haloperidol- Metabolism of Chloroquine decreases when combined. Phenytoin- Metabolism of Phenytoin can be decreased when combined. Hydroxychloroquine- The metabolism of Chloroquine decreases when combined.
Hesperidin	Used for the treatment of venous diseases that affect blood vessels - hemorrhoids, varicose veins, venous stasis, etc.	No Data Available	No Data Available	Oral but No Data Available for dosage	No Data Available
Inosine	Multiple sclerosis and Parkinson's disease	No Data Available	Neuroprotective, cardioprotective, anti-inflammatory, and immunomodulatory activities.	Extracorporeal but No Data Available for dosage	No Data Available
Phenytoin	Anticonvulsant	Affects cardiovascular and nervous system. Slurred speech, tremor, nausea, vomiting, ataxia. Can cause AV and SA blocks, dysrhythmia.	Acts as an anticonvulsant. The fraction of unbound phenytoin is able to produce the effect of an anticonvulsant.	Oral - 100 mg	Paclitaxel-The serum concentration of Paclitaxel can be decreased Anastrozole- Metabolism of Phenytoin decreases when combined. Heparin- Therapeutic efficacy of Heparin can be increased when Haloperidol- Metabolism of Haloperidol decreases when combined with Phenytoin. Doxifluridine- Serum concentration of Phenytoin increases when combined. Chloroquine- Metabolism of Phenytoin decreases when combined. Hydroxychloroquine- The Therapeutic efficacy of Phenytoin decreases when combined.
Crocin	Treatment of hyperglycemia, metabolic syndrome, hypertriglyceridemia, and hypercholesterolemia.	No Data Available	No Data Available	No Data Available	No Data Available

Hydroxy-chloroquine	Malaria treatment and prevention	Headache, drowsiness, visual disturbances. Respiratory and cardiac arrest may arise.	Affects the function of lysosomes in plasmodia and humans. Reduces low affinity self antigen presentation in autoimmune diseases. Interferes with the ability of plasmodia to use hemoglobin for energy.	Oral - 200mg/1	Paclitaxel-The risk or severity of adverse effects can be increased Haloperidol- Metabolism of Haloperidol can be decreased when combined with Doxifluridine- Risk or severity of adverse effects can increase when combined. Phenytoin- The Therapeutic efficacy of Phenytoin decreases when combined with Hydroxychloroquine.
---------------------	----------------------------------	--	--	----------------	---

Known Mechanism of Action of drugs from approved libraries. Understanding the mechanism of action for each repurposable drug is important in predicting if the compound will be capable of combating COVID-19. To enable identification of drugs suitable for combination therapies, we have assembled mechanisms of action for each drug from current indications and from the Drug Bank. This information in addition to our current findings will provide key guidance regarding which compounds are likely to show effectiveness in blocking target proteins and suppressing this new coronavirus. **Table 10** presents the mechanism of action for the following repurposable drug compounds that were screened from the ZINC database.

Known drug-drug interactions of leads from approved libraries. While understanding the mechanism of action and pharmacodynamics of each drug compound is important, combination therapy requires an understanding of potential drug-drug interactions. Listed in Table 10 is a compilation of the drugs screened from the ZINC library and their respective interactions with the other compounds. Each interaction listed exhibits the effect that the host drug has in terms of metabolism or other side effects that could take place. For the drug compounds that do not have other compounds listed, data was unavailable. The data was gathered from DrugBank¹⁵⁷.

For the drugs mentioned in Table 10, the possibility of combination therapy offers benefits and as well has highlighting which drugs could have a negative effect when used with others. For hydroxychloroquine, a drug that has received attention as a potential therapeutic to COVID-19, we have gathered data of its effect in combination therapy with other compounds that have been screened. When used in combination with Paclitaxel and Doxifluridine, the risks associated with each compound can increase, potentially leading to complications or even death. The drugs in Table X show which compounds should benefit from combination therapy and which likely will not. Understanding the dynamics of combination therapy and the compounds listed will better help combat COVID-19 and to understand the drug compounds in use.

CONCLUSION

The rapid spread of SARS-CoV-2 continues to create havoc in health systems and economies, affected every nation in the world. As this is a novel coronavirus, there are no vaccines currently available, though they are being developed at an unprecedented pace and we must resort to small molecule therapeutics against COVID-19. There has been an international focus on the potential efficacy of repurposable drug candidates including remdesivir and hydroxychloroquine, among others. With each controlled clinical study that comes out, it becomes more evident that nations were too quick to push certain compounds, consequently reducing the supply to patients who needed them to treat other already indicated diseases. There is a possibility that these previously mentioned compounds may still have a place in the clinical realm as a treatment for COVID-19, but not as stand-alone therapies as currently utilized. It is clear that until a SARS-CoV-2 specific compound is developed and clinically approved, the best way is to find treatment through a multifaceted approach. This philosophy is at the forefront of our work, first by screening approved compounds for repurposing potential, and by identifying the best possible combinations providing a multifaceted attack on SARS-CoV-2. In this context, we commenced a CAAD through HTVS approach using

large pool of world approved drug libraries to identify potential drugs for immediate deployment. Our *in-silico* studies have identified a series of repurposable drugs that can be utilized in clinical trials. Our study also outlined the primary mechanism of action of these drugs which can further aid clinical trial designs to investigate combinations of compounds that have individually failed to treat COVID-19. It is important to note that caution must be taken with some of these drugs, especially the anti-oncolytic and anti-psychotics that can have severe adverse effects in the context of their utility as antivirals. Also, special notice must be taken with compounds such as crocin, haloperidol glucuronide, doxifluridine, ivermectin, anastrozole, XAV-939, isoquercetin, and phenytoin, that these drugs would be expected to be administered in lower doses than what is normally administered for their original indications. We predict that these drugs will not suffice as candidates that may have stand-alone efficacy in treating COVID-19. Rather, these compounds should be tested in combinatorial studies as an additive to a drug with lower toxicity to the host as a potential treatment with synergistic efficacies.

Application of our multi-pronged drug discovery approach is consistent with the WHO's desire to repurpose approved drugs that have acceptable safety profiles. Our study further highlights that target-based drug repurposing is a promising strategy, specifically in helping predict the best combination therapy to avoid the limitations of suboptimal performance by individual drugs. Furthermore, implementation of this approach should be an effective method to pre-select approved drug(s) for clinical testing and evaluation for clinical use. The advantage of using this approach relative to developing new drugs is a potentially vast savings of both cost and time. If any of these approved compounds are safe and effective in patients, then this may significantly alter the degree of infectivity of SARS-CoV-2 and/or the duration of COVID-19 illness in the coming months and years.

Acknowledgements

Authors sincerely thank the Department of Medicine, Loyola University Medical Center and Stritch School of Medicine for providing the funding support for the Drug Discovery Program, software acquisition and the High Computing Platform.

Disclosure

The authors declare no competing financial interests.

Author Contributions

YG and PK designed the study and performed *in-silico* analysis. DM, RM, CMP, DJI and HH assisted in data mining, virtual screening, related *in-silico* analysis and table generations for drug characteristics. DM, CMP and YG covered the epidemiology, virus, genome and target proteins background. PK, AB and RD contributed to clinical aspects of the study. DB, YG and BR contributed chemical and molecular aspects of leads. AH, SB and JMD helped with the mechanistic aspects and usability and of the drug library and *in-vitro* testing. All authors rigorously edited the manuscript.

REFERENCES

- (1) Huang, C.; Wang, Y.; Li, X.; Ren, L.; Zhao, J.; Hu, Y.; Zhang, L.; Fan, G.; Xu, J.; Gu, X.; others. Clinical Features of Patients Infected with 2019 Novel Coronavirus in Wuhan, China. *The Lancet* **2020**, 395 (10223), 497–506.
- (2) Lu, R.; Zhao, X.; Li, J.; Niu, P.; Yang, B.; Wu, H.; Wang, W.; Song, H.; Huang, B.; Zhu, N.; others. Genomic Characterisation and Epidemiology of 2019 Novel Coronavirus: Implications for Virus Origins and Receptor Binding. *The Lancet* **2020**, 395 (10224), 565–574.
- (3) Organization, W. H.; others. Coronavirus Disease 2019 (COVID-19): Situation Report, 85. **2020**.
- (4) Dong, E.; Du, H.; Gardner, L. An Interactive Web-Based Dashboard to Track COVID-19 in Real Time. *Lancet Infect. Dis.* **2020**.
- (5) Phan, L. T.; Nguyen, T. V.; Luong, Q. C.; Nguyen, T. V.; Nguyen, H. T.; Le, H. Q.; Nguyen, T. T.; Cao, T. M.; Pham, Q. D. Importation and Human-to-Human Transmission of a Novel Coronavirus in Vietnam. *N. Engl. J. Med.* **2020**, 382 (9), 872–874.
- (6) Chan, J. F.-W.; Yuan, S.; Kok, K.-H.; To, K. K.-W.; Chu, H.; Yang, J.; Xing, F.; Liu, J.; Yip, C. C.-Y.; Poon, R. W.-S.; others. A Familial Cluster of Pneumonia Associated with the 2019 Novel Coronavirus Indicating Person-to-Person Transmission: A Study of a Family Cluster. *The Lancet* **2020**, 395 (10223), 514–523.
- (7) Zhang, W.; Du, R.-H.; Li, B.; Zheng, X.-S.; Yang, X.-L.; Hu, B.; Wang, Y.-Y.; Xiao, G.-F.; Yan, B.; Shi, Z.-L.; others. Molecular and Serological Investigation of 2019-NCov Infected Patients: Implication of Multiple Shedding Routes. *Emerg. Microbes Infect.* **2020**, 9 (1), 386–389.
- (8) Zhong, N.; Zheng, B.; Li, Y.; Poon, L.; Xie, Z.; Chan, K.; Li, P.; Tan, S.; Chang, Q.; Xie, J.; others. Epidemiology and Cause of Severe Acute Respiratory Syndrome (SARS) in Guangdong, People's Republic of China, in February, 2003. *The Lancet* **2003**, 362 (9393), 1353–1358.
- (9) Guan, Y.; Peiris, J.; Zheng, B.; Poon, L.; Chan, K.; Zeng, F.; Chan, C.; Chan, M.; Chen, J.; Chow, K.; others. Molecular Epidemiology of the Novel Coronavirus That Causes Severe Acute Respiratory Syndrome. *The Lancet* **2004**, 363 (9403), 99–104.
- (10) Zaki, A.; van Boheemen, S.; Bestebroer, T.; Osterhaus, A.; Fouchier, R. 365 2012. Isolation of a Novel Coronavirus from a Man with Pneumonia in Saudi Arabia. *N* **366**, 1814–1820.
- (11) Paules, C. I.; Marston, H. D.; Fauci, A. S. Coronavirus Infections—More than Just the Common Cold. *Jama* **2020**, 323 (8), 707–708.
- (12) Committee, L. I. I.; others. Korea Centers for Disease Control and Prevention. *Rep. Incid. Humidifier Disinfect.-Assoc. Damages Seoul Han Rim Won Publ.* **2014**, 39.
- (13) Chowell, G.; Abdirizak, F.; Lee, S.; Lee, J.; Jung, E.; Nishiura, H.; Viboud, C. Transmission Characteristics of MERS and SARS in the Healthcare Setting: A Comparative Study. *BMC Med.* **2015**, 13 (1), 210.
- (14) Hunter, J. C.; Nguyen, D.; Aden, B.; Al Bandar, Z.; Al Dhaheri, W.; Elkheir, K. A.; Khudair, A.; Al Mulla, M.; El Saleh, F.; Imambaccus, H.; others. Transmission of Middle East Respiratory Syndrome Coronavirus Infections in Healthcare Settings, Abu Dhabi. *Emerg. Infect. Dis.* **2016**, 22 (4), 647.
- (15) Lai, C.-C.; Shih, T.-P.; Ko, W.-C.; Tang, H.-J.; Hsueh, P.-R. Severe Acute Respiratory Syndrome Coronavirus 2 (SARS-CoV-2) and Corona Virus Disease-2019 (COVID-19): The Epidemic and the Challenges. *Int. J. Antimicrob. Agents* **2020**, 105924.
- (16) Anderson, R. M.; Fraser, C.; Ghani, A. C.; Donnelly, C. A.; Riley, S.; Ferguson, N. M.; Leung, G. M.; Lam, T. H.; Hedley, A. J. Epidemiology, Transmission Dynamics and

- Control of SARS: The 2002–2003 Epidemic. *Philos. Trans. R. Soc. Lond. B. Biol. Sci.* **2004**, 359 (1447), 1091–1105.
- (17) Cowling, B. J.; Park, M.; Fang, V. J.; Wu, P.; Leung, G. M.; Wu, J. T. Preliminary Epidemiologic Assessment of MERS-CoV Outbreak in South Korea, May–June 2015. *Euro Surveill. Bull. Eur. Sur Mal. Transm. Eur. Commun. Dis. Bull.* **2015**, 20 (25).
 - (18) Peiris, J.; Lai, S.; Poon, L.; Guan, Y.; Yam, L.; Lim, W.; Nicholls, J.; Yee, W.; Yan, W.; Cheung, M.; others. Coronavirus as a Possible Cause of Severe Acute Respiratory Syndrome. *The Lancet* **2003**, 361 (9366), 1319–1325.
 - (19) de Wit, E.; van Doremalen, N.; Falzarano, D.; Munster, V. J. SARS and MERS: Recent Insights into Emerging Coronaviruses. *Nat. Rev. Microbiol.* **2016**, 14 (8), 523.
 - (20) Zou, L.; Ruan, F.; Huang, M.; Liang, L.; Huang, H.; Hong, Z.; Yu, J.; Kang, M.; Song, Y.; Xia, J.; others. SARS-CoV-2 Viral Load in Upper Respiratory Specimens of Infected Patients. *N. Engl. J. Med.* **2020**, 382 (12), 1177–1179.
 - (21) Masters, P. S. Coronavirus Genomic RNA Packaging. *Virology* **2019**.
 - (22) Pradesh, U.; Upadhyay, P. D. D.; Vigyan, P. C. Coronavirus Infection in Equines: A Review. *Asian J Anim Vet Adv* **2014**, 9 (3), 164–176.
 - (23) Ahmad, T.; Rodriguez-Morales, A. J. Emergence of COVID-19 (Formerly 2019-Novel Coronavirus): A New Threat from China. *Rev. Panam. Enfermedades Infecc.* **2020**, 37–38.
 - (24) Zumla, A.; Hui, D. S.; Perlman, S. Middle East Respiratory Syndrome. *The Lancet* **2015**, 386 (9997), 995–1007.
 - (25) van Boheemen, S.; de Graaf, M.; Lauber, C.; Bestebroer, T. M.; Raj, V. S.; Zaki, A. M.; Osterhaus, A. D.; Haagmans, B. L.; Gorbalenya, A. E.; Snijder, E. J.; others. Genomic Characterization of a Newly Discovered Coronavirus Associated with Acute Respiratory Distress Syndrome in Humans. *MBio* **2012**, 3 (6), e00473-12.
 - (26) Agostini, M. L.; Andres, E. L.; Sims, A. C.; Graham, R. L.; Sheahan, T. P.; Lu, X.; Smith, E. C.; Case, J. B.; Feng, J. Y.; Jordan, R.; others. Coronavirus Susceptibility to the Antiviral Remdesivir (GS-5734) Is Mediated by the Viral Polymerase and the Proofreading Exoribonuclease. *MBio* **2018**, 9 (2), e00221–18.
 - (27) Liu, W.; Morse, J. S.; Lalonde, T.; Xu, S. Learning from the Past: Possible Urgent Prevention and Treatment Options for Severe Acute Respiratory Infections Caused by 2019-NCoV. *Chembiochem* **2020**.
 - (28) Guo, D. Old Weapon for New Enemy: Drug Repurposing for Treatment of Newly Emerging Viral Diseases. *Virol. Sin.* **2020**, 1–3.
 - (29) Maxmen, A. More than 80 Clinical Trials Launch to Test Coronavirus Treatments. *Nature* **2020**, 578 (7795), 347.
 - (30) Mifsud, E. J.; Hayden, F. G.; Hurt, A. C. Antivirals Targeting the Polymerase Complex of Influenza Viruses. *Antiviral Res.* **2019**, 104545.
 - (31) Warren, T. K.; Jordan, R.; Lo, M. K.; Ray, A. S.; Mackman, R. L.; Soloveva, V.; Siegel, D.; Perron, M.; Bannister, R.; Hui, H. C.; others. Therapeutic Efficacy of the Small Molecule GS-5734 against Ebola Virus in Rhesus Monkeys. *Nature* **2016**, 531 (7594), 381–385.
 - (32) Sheahan, T. P.; Sims, A. C.; Leist, S. R.; Schäfer, A.; Won, J.; Brown, A. J.; Montgomery, S. A.; Hogg, A.; Babusis, D.; Clarke, M. O.; others. Comparative Therapeutic Efficacy of Remdesivir and Combination Lopinavir, Ritonavir, and Interferon Beta against MERS-CoV. *Nat. Commun.* **2020**, 11 (1), 1–14.
 - (33) Lin, S.; Shen, R.; He, J.; Li, X.; Guo, X. Molecular Modeling Evaluation of the Binding Effect of Ritonavir, Lopinavir and Darunavir to Severe Acute Respiratory Syndrome Coronavirus 2 Proteases. *bioRxiv* **2020**.

- (34) Zhou, Y.; Vedantham, P.; Lu, K.; Agudelo, J.; Carrion Jr, R.; Nunneley, J. W.; Barnard, D.; Pöhlmann, S.; McKerrow, J. H.; Renslo, A. R.; others. Protease Inhibitors Targeting Coronavirus and Filovirus Entry. *Antiviral Res.* **2015**, *116*, 76–84.
- (35) Kumar, V.; Shin, J. S.; Shie, J.-J.; Ku, K. B.; Kim, C.; Go, Y. Y.; Huang, K.-F.; Kim, M.; Liang, P.-H. Identification and Evaluation of Potent Middle East Respiratory Syndrome Coronavirus (MERS-CoV) 3CLPro Inhibitors. *Antiviral Res.* **2017**, *141*, 101–106.
- (36) Anand, K.; Ziebuhr, J.; Wadhwani, P.; Mesters, J. R.; Hilgenfeld, R. Coronavirus Main Proteinase (3CLpro) Structure: Basis for Design of Anti-SARS Drugs. *Science* **2003**, *300* (5626), 1763–1767.
- (37) Info, A. Guidelines for the Use of Antiretroviral Agents in HIV-1-Infected Adults and Adolescents. *Panel Antiretrovir. Guidel. Adults Adolesc. Ser. Online Available Httpwww Aidsinfo Nih Govcontentfiles/vguidelinesadultandadolescentgl Pdf Accessed* **2013**, *15*.
- (38) Ortiz-Alcantara, J.; others. Small Molecule Inhibitors of the SARS-CoV Nsp15 Endoribonuclease. *Virus Adapt. Treat.* **2010**, *2*, 125–133.
- (39) Richardson, P.; Griffin, I.; Tucker, C.; Smith, D.; Oechsle, O.; Phelan, A.; Stebbing, J. Baricitinib as Potential Treatment for 2019-NCov Acute Respiratory Disease. *Lancet Lond. Engl.* **2020**, *395* (10223), e30.
- (40) Vincent, M. J.; Bergeron, E.; Benjannet, S.; Erickson, B. R.; Rollin, P. E.; Ksiazek, T. G.; Seidah, N. G.; Nichol, S. T. Chloroquine Is a Potent Inhibitor of SARS Coronavirus Infection and Spread. *Virol. J.* **2005**, *2* (1), 69.
- (41) Hoffmann, M.; Kleine-Weber, H.; Schroeder, S.; Krüger, N.; Herrler, T.; Erichsen, S.; Schiergens, T. S.; Herrler, G.; Wu, N.-H.; Nitsche, A.; others. SARS-CoV-2 Cell Entry Depends on ACE2 and TMPRSS2 and Is Blocked by a Clinically Proven Protease Inhibitor. *Cell* **2020**.
- (42) Wu, Y. Compensation of ACE2 Function for Possible Clinical Management of 2019-NCov-Induced Acute Lung Injury. *Virol. Sin.* **2020**, 1–3.
- (43) Baker, N. C.; Ekins, S.; Williams, A. J.; Tropsha, A. A Bibliometric Review of Drug Repurposing. *Drug Discov. Today* **2018**, *23* (3), 661–672.
- (44) Organization, W. H.; others. Coronavirus Disease 2019 (COVID-19): Situation Report, 85. **2020**.
- (45) de Wit, E.; Feldmann, F.; Cronin, J.; Jordan, R.; Okumura, A.; Thomas, T.; Scott, D.; Cihlar, T.; Feldmann, H. Prophylactic and Therapeutic Remdesivir (GS-5734) Treatment in the Rhesus Macaque Model of MERS-CoV Infection. *Proc. Natl. Acad. Sci.* **2020**, *117* (12), 6771–6776.
- (46) Mulangu, S.; Dodd, L. E.; Davey Jr, R. T.; Tshiani Mbaya, O.; Proschan, M.; Mukadi, D.; Lusakibanza Manzo, M.; Nzolo, D.; Tshomba Oloma, A.; Ibanda, A.; others. A Randomized, Controlled Trial of Ebola Virus Disease Therapeutics. *N. Engl. J. Med.* **2019**, *381* (24), 2293–2303.
- (47) Cao, B.; Wang, Y.; Wen, D.; Liu, W.; Wang, J.; Fan, G.; Ruan, L.; Song, B.; Cai, Y.; Wei, M.; others. A Trial of Lopinavir–Ritonavir in Adults Hospitalized with Severe Covid-19. *N. Engl. J. Med.* **2020**.
- (48) Inglot, A. D. Comparison of the Antiviral Activity in Vitro of Some Non-Steroidal Anti-Inflammatory Drugs. *J. Gen. Virol.* **1969**, *4* (2), 203–214.
- (49) of the International, C. S. G.; others. The Species Severe Acute Respiratory Syndrome-Related Coronavirus: Classifying 2019-NCov and Naming It SARS-CoV-2. *Nat. Microbiol.* **2020**, 1.
- (50) Zhang, T.; Wu, Q.; Zhang, Z. Probable Pangolin Origin of SARS-CoV-2 Associated with the COVID-19 Outbreak. *Curr. Biol.* **2020**.
- (51) Davidson, A. D.; Williamson, M. K.; Lewis, S.; Shoemark, D.; Carroll, M. W.; Heesom, K.; Zambon, M.; Ellis, J.; Lewis, P. A.; Hiscox, J. A.; others. Characterisation of the Transcriptome and Proteome of SARS-CoV-2 Using Direct RNA Sequencing and

- Tandem Mass Spectrometry Reveals Evidence for a Cell Passage Induced in-Frame Deletion in the Spike Glycoprotein That Removes the Furin-like Cleavage Site. *BioRxiv* **2020**.
- (52) Astuti, I.; others. Severe Acute Respiratory Syndrome Coronavirus 2 (SARS-CoV-2): An Overview of Viral Structure and Host Response. *Diabetes Metab. Syndr. Clin. Res. Rev.* **2020**.
 - (53) Barretto, N.; Jukneliene, D.; Ratia, K.; Chen, Z.; Mesecar, A. D.; Baker, S. C. The Papain-like Protease of Severe Acute Respiratory Syndrome Coronavirus Has Deubiquitinating Activity. *J. Virol.* **2005**, *79* (24), 15189–15198.
 - (54) Chen, Y.; Cai, H.; Xiang, N.; Tien, P.; Ahola, T.; Guo, D.; others. Functional Screen Reveals SARS Coronavirus Nonstructural Protein Nsp14 as a Novel Cap N7 Methyltransferase. *Proc. Natl. Acad. Sci.* **2009**, *106* (9), 3484–3489.
 - (55) Minskaia, E.; Hertzog, T.; Gorbalenya, A. E.; Campanacci, V.; Cambillau, C.; Canard, B.; Ziebuhr, J. Discovery of an RNA Virus 3'→ 5' Exoribonuclease That Is Critically Involved in Coronavirus RNA Synthesis. *Proc. Natl. Acad. Sci.* **2006**, *103* (13), 5108–5113.
 - (56) Bouvet, M.; Debarnot, C.; Imbert, I.; Selisko, B.; Snijder, E. J.; Canard, B.; Decroly, E. In Vitro Reconstitution of SARS-Coronavirus MRNA Cap Methylation. *PLoS Pathog.* **2010**, *6* (4).
 - (57) Wang, Y.; Sun, Y.; Wu, A.; Xu, S.; Pan, R.; Zeng, C.; Jin, X.; Ge, X.; Shi, Z.; Ahola, T.; others. Coronavirus Nsp10/Nsp16 Methyltransferase Can Be Targeted by Nsp10-Derived Peptide in Vitro and in Vivo to Reduce Replication and Pathogenesis. *J. Virol.* **2015**, *89* (16), 8416–8427.
 - (58) Daffis, S.; Szretter, K. J.; Schriewer, J.; Li, J.; Youn, S.; Errett, J.; Lin, T.-Y.; Schneller, S.; Zust, R.; Dong, H.; others. 2'-O Methylation of the Viral MRNA Cap Evades Host Restriction by IFIT Family Members. *Nature* **2010**, *468* (7322), 452–456.
 - (59) Züst, R.; Cervantes-Barragan, L.; Habjan, M.; Maier, R.; Neuman, B. W.; Ziebuhr, J.; Szretter, K. J.; Baker, S. C.; Barchet, W.; Diamond, M. S.; others. Ribose 2'-O-Methylation Provides a Molecular Signature for the Distinction of Self and Non-Self MRNA Dependent on the RNA Sensor Mda5. *Nat. Immunol.* **2011**, *12* (2), 137.
 - (60) Eckerle, L. D.; Lu, X.; Sperry, S. M.; Choi, L.; Denison, M. R. High Fidelity of Murine Hepatitis Virus Replication Is Decreased in Nsp14 Exoribonuclease Mutants. *J. Virol.* **2007**, *81* (22), 12135–12144.
 - (61) Ivanov, K. A.; Thiel, V.; Dobbe, J. C.; van der Meer, Y.; Snijder, E. J.; Ziebuhr, J. Multiple Enzymatic Activities Associated with Severe Acute Respiratory Syndrome Coronavirus Helicase. *J. Virol.* **2004**, *78* (11), 5619–5632.
 - (62) Imbert, I.; Ulferts, R.; Ziebuhr, J.; Canard, B. SARS Coronavirus Replicative Enzymes: Structures and Mechanisms. In *Molecular biology of the SARS-Coronavirus*; Springer, 2010; pp 99–114.
 - (63) Zhang, L.; Li, L.; Yan, L.; Ming, Z.; Jia, Z.; Lou, Z.; Rao, Z. Structural and Biochemical Characterization of Endoribonuclease Nsp15 Encoded by Middle East Respiratory Syndrome Coronavirus. *J. Virol.* **2018**, *92* (22), e00893–18.
 - (64) Baig, K. M. SITE DIRECTED MUTAGENESIS OF SEVERE ACUTE RESPIRATORY SYNDROME (SARS) CORONAVIRUS NSP 15 ENDORIBONUCLEASE. PhD Thesis, 2006.
 - (65) Bhardwaj, K.; Guarino, L.; Kao, C. C. The Severe Acute Respiratory Syndrome Coronavirus Nsp15 Protein Is an Endoribonuclease That Prefers Manganese as a Cofactor. *J. Virol.* **2004**, *78* (22), 12218–12224.
 - (66) Lei, Y.; Moore, C. B.; Liesman, R. M.; O'Connor, B. P.; Bergstralh, D. T.; Chen, Z. J.; Pickles, R. J.; Ting, J. P.-Y. MAVS-Mediated Apoptosis and Its Inhibition by Viral Proteins. *PloS One* **2009**, *4* (5).

- (67) Menachery, V. D.; Gralinski, L. E.; Mitchell, H. D.; Dinnon, K. H.; Leist, S. R.; Yount, B. L.; Graham, R. L.; McAnarney, E. T.; Stratton, K. G.; Cockrell, A. S.; others. Middle East Respiratory Syndrome Coronavirus Nonstructural Protein 16 Is Necessary for Interferon Resistance and Viral Pathogenesis. *mSphere* **2017**, 2 (6), e00346–17.
- (68) Menachery, V. D.; Yount, B. L.; Josset, L.; Gralinski, L. E.; Scobey, T.; Agnihothram, S.; Katze, M. G.; Baric, R. S. Attenuation and Restoration of Severe Acute Respiratory Syndrome Coronavirus Mutant Lacking 2'-O-Methyltransferase Activity. *J. Virol.* **2014**, 88 (8), 4251–4264.
- (69) Adedeji, A. O.; Singh, K.; Sarafianos, S. G. Structural and Biochemical Basis for the Difference in the Helicase Activity of Two Different Constructs of SARS-CoV Helicase. *Cell. Mol. Biol. Noisy--Gd. Fr.* **2012**, 58 (1), 114.
- (70) Yu, M.-S.; Lee, J.; Lee, J. M.; Kim, Y.; Chin, Y.-W.; Jee, J.-G.; Keum, Y.-S.; Jeong, Y.-J. Identification of Myricetin and Scutellarein as Novel Chemical Inhibitors of the SARS Coronavirus Helicase, Nsp13. *Bioorg. Med. Chem. Lett.* **2012**, 22 (12), 4049–4054.
- (71) Shu, T.; Huang, M.; Wu, D.; Ren, Y.; Zhang, X.; Han, Y.; Mu, J.; Wang, R.; Qiu, Y.; Zhang, D.-Y.; others. SARS-Coronavirus-2 Nsp13 Possesses NTPase and RNA Helicase Activities.
- (72) Peng, Q.; Peng, R.; Yuan, B.; Zhao, J.; Wang, M.; Wang, X.; Wang, Q.; Sun, Y.; Fan, Z.; Qi, J.; others. Structural and Biochemical Characterization of Nsp12-Nsp7-Nsp8 Core Polymerase Complex from COVID-19 Virus. *bioRxiv* **2020**.
- (73) Kirchdoerfer, R. N.; Ward, A. B. Structure of the SARS-CoV Nsp12 Polymerase Bound to Nsp7 and Nsp8 Co-Factors. *Nat. Commun.* **2019**, 10 (1), 1–9.
- (74) Yap, Y.; Zhang, X.; Andonov, A.; He, R. Structural Analysis of Inhibition Mechanisms of Aurintricarboxylic Acid on SARS-CoV Polymerase and Other Proteins. *Comput. Biol. Chem.* **2005**, 29 (3), 212–219.
- (75) Posthuma, C. C.; te Velthuis, A. J.; Snijder, E. J. Nidovirus RNA Polymerases: Complex Enzymes Handling Exceptional RNA Genomes. *Virus Res.* **2017**, 234, 58–73.
- (76) Ju, J.; Li, X.; Kumar, S.; Jockusch, S.; Chien, M.; Tao, C.; Morozova, I.; Kalachikov, S.; Kirchdoerfer, R.; Russo, J. J. Nucleotide Analogues as Inhibitors of SARS-CoV Polymerase. *bioRxiv* **2020**.
- (77) Zhang, C.; Zheng, W.; Huang, X.; Bell, E. W.; Zhou, X.; Zhang, Y. Protein Structure and Sequence Re-Analysis of 2019-NCoV Genome Does Not Indicate Snakes as Its Intermediate Host or the Unique Similarity between Its Spike Protein Insertions and HIV-1. *ArXiv Prepr. ArXiv200203173* **2020**.
- (78) Wu, Q.; Peng, Z.; Zhang, Y.; Yang, J. COACH-D: Improved Protein–Ligand Binding Sites Prediction with Refined Ligand-Binding Poses through Molecular Docking. *Nucleic Acids Res.* **2018**, 46 (W1), W438–W442.
- (79) Roos, K.; Wu, C.; Damm, W.; Reboul, M.; Stevenson, J. M.; Lu, C.; Dahlgren, M. K.; Mondal, S.; Chen, W.; Wang, L.; others. OPLS3e: Extending Force Field Coverage for Drug-like Small Molecules. *J. Chem. Theory Comput.* **2019**, 15 (3), 1863–1874.
- (80) Friesner, R. A.; Murphy, R. B.; Repasky, M. P.; Frye, L. L.; Greenwood, J. R.; Halgren, T. A.; Sanschagrin, P. C.; Mainz, D. T. Extra Precision Glide: Docking and Scoring Incorporating a Model of Hydrophobic Enclosure for Protein- Ligand Complexes. *J. Med. Chem.* **2006**, 49 (21), 6177–6196.
- (81) Aiyer, P. V. Amylases and Their Applications. *Afr. J. Biotechnol.* **2005**, 4 (13).
- (82) Takasaki, Y.; Shinohara, H.; Tsuruhisa, M.; Hayashi, S.; Imada, K. Maltotetraose-Producing Amylase from *Bacillus* Sp. MG-4. *Agric. Biol. Chem.* **1991**, 55 (7), 1715–1720.
- (83) Abdullaev, F. I. Cancer Chemopreventive and Tumorcidal Properties of Saffron (*Crocus Sativus* L.). *Exp. Biol. Med.* **2002**, 227 (1), 20–25.

- (84) Stern, S. A.; Zink, B.; Wang, X.; Mertz, M. The Effects of Resuscitation with Trans-Sodium Crocetin in a Model of Combined Hemorrhagic Shock and Traumatic Brain Injury. *Acad. Emerg. Med.* **2002**, 9 (5), 415.
- (85) Tseng, T.-H.; Chu, C.-Y.; Huang, J.-M.; Shiow, S.-J.; Wang, C.-J. Crocetin Protects against Oxidative Damage in Rat Primary Hepatocytes. *Cancer Lett.* **1995**, 97 (1), 61–67.
- (86) Brito, D. A.; Yang, Z.; Rieder, C. L. Microtubules Do Not Promote Mitotic Slippage When the Spindle Assembly Checkpoint Cannot Be Satisfied. *J. Cell Biol.* **2008**, 182 (4), 623–629.
- (87) Rowinsky, E. K., MD. The Development and Clinical Utility of the Taxane Class of Antimicrotubule Chemotherapy Agents. *Annu. Rev. Med.* **1997**, 48 (1), 353–374.
- (88) Zhou, J.; Zhong, D.-W.; Wang, Q.-W.; Miao, X.-Y.; Xu, X.-D. Paclitaxel Ameliorates Fibrosis in Hepatic Stellate Cells via Inhibition of TGF- β /Smad Activity. *World J. Gastroenterol. WJG* **2010**, 16 (26), 3330.
- (89) Sun, L.; Zhang, D.; Liu, F.; Xiang, X.; Ling, G.; Xiao, L.; Liu, Y.; Zhu, X.; Zhan, M.; Yang, Y.; others. Low-Dose Paclitaxel Ameliorates Fibrosis in the Remnant Kidney Model by down-Regulating MiR-192. *J. Pathol.* **2011**, 225 (3), 364–377.
- (90) Tepe, G.; Zeller, T.; Albrecht, T.; Heller, S.; Schwarzwälder, U.; Beregi, J.-P.; Claussen, M. C. D.; Oldenburg, A.; Scheller, B.; Speck, U. Local Delivery of Paclitaxel to Inhibit Restenosis during Angioplasty of the Leg. *N. Engl. J. Med.* **2008**, 358 (7), 689–699.
- (91) Tang, N.; Bai, H.; Chen, X.; Gong, J.; Li, D.; Sun, Z. Anticoagulant Treatment Is Associated with Decreased Mortality in Severe Coronavirus Disease 2019 Patients with Coagulopathy. *J. Thromb. Haemost.* **2020**.
- (92) Shi, C.; Wang, C.; Wang, H.; Yang, C.; Cai, F.; Zeng, F.; Cheng, F.; Liu, Y.; Zhou, T.; Deng, B.; others. The Potential of Low Molecular Weight Heparin to Mitigate Cytokine Storm in Severe COVID-19 Patients: A Retrospective Clinical Study. *medRxiv* **2020**.
- (93) Negri, E. M.; Piloto, B.; Morinaga, L. K.; Jardim, C. V. P.; Lamy, S. A. E.-D.; Ferreira, M. A.; D'Amico, E. A.; Deheinzelin, D. Heparin Therapy Improving Hypoxia in COVID-19 Patients-a Case Series. *medRxiv* **2020**.
- (94) Ehsani, S. Distant Sequence Similarity between Hepcidin and the Novel Coronavirus Spike Glycoprotein: A Potential Hint at the Possibility of Local Iron Dysregulation in COVID-19. *ArXiv Prepr. ArXiv200312191* **2020**.
- (95) Poli, M.; Girelli, D.; Campostrini, N.; Maccarinelli, F.; Finazzi, D.; Lusciati, S.; Nai, A.; Arosio, P. Heparin: A Potent Inhibitor of Hepcidin Expression in Vitro and in Vivo. *Blood J. Am. Soc. Hematol.* **2011**, 117 (3), 997–1004.
- (96) Kim, H.; Lee, M.-K.; Ko, J.; Park, C.-J.; Kim, M.; Jeong, Y.; Hong, S.; Varani, G.; Choi, B.-S. Aminoglycoside Antibiotics Bind to the Influenza A Virus RNA Promoter. *Mol. Biosyst.* **2012**, 8 (11), 2857–2859.
- (97) Manvar, D.; Pandey, N.; Pandey, V. N. Anti-HCV Drug Development. *Abstr. Res.* **2011**, 90, A21–A78.
- (98) Ruttloff, H.; Täufel, A.; Krause, W.; Haenel, H.; Täufel, K. Die Intestinal-Enzymatische Spaltung von Galakto-Oligosacchariden Im Darm von Tier Und Mensch Mit Besonderer Berücksichtigung von Lactobacillus Bifidus 2. Mitt. Zum Intestinalen Verhalten Der Lactulose. *Food/Nahrung* **1967**, 11 (1), 39–46.
- (99) Hu, G. Neomycin Inhibits the Angiogenic Activity of Fibroblast and Epidermal Growth Factors. *Biochem. Biophys. Res. Commun.* **2001**, 287 (4), 870–874.
- (100) Kishimoto, K.; Yoshida, S.; Ibaragi, S.; Yoshioka, N.; HU, G.-F.; Sasaki, A. Neamine Inhibits Oral Cancer Progression by Suppressing Angiogenin-Mediated Angiogenesis and Cancer Cell Proliferation. *Anticancer Res.* **2014**, 34 (5), 2113–2121.

- (101) Lounis, N.; Ji, B.; Truffot-Pernot, C.; Grosset, J. Which Aminoglycoside or Fluoroquinolone Is More Active against Mycobacterium Tuberculosis in Mice? *Antimicrob. Agents Chemother.* **1997**, *41* (3), 607–610.
- (102) Yamaguchi, M.; Eda, J.; Kobayashi, F.; Mitsunashi, S. Mode of Action of Lividomycin on Protein Synthesis in Escherichia Coli. *Antimicrob. Agents Chemother.* **1973**, *4* (3), 380–382.
- (103) Robidoux, A.; Tang, G.; Rastogi, P.; Geyer Jr, C. E.; Azar, C. A.; Atkins, J. N.; Fehrenbacher, L.; Bear, H. D.; Baez-Diaz, L.; Sarwar, S.; others. Lapatinib as a Component of Neoadjuvant Therapy for HER2-Positive Operable Breast Cancer (NSABP Protocol B-41): An Open-Label, Randomised Phase 3 Trial. *Lancet Oncol.* **2013**, *14* (12), 1183–1192.
- (104) Alba, E.; Albanell, J.; De La Haba, J.; Barnadas, A.; Calvo, L.; Sanchez-Rovira, P.; Ramos, M.; Rojo, F.; Burgues, O.; Carrasco, E.; others. Trastuzumab or Lapatinib with Standard Chemotherapy for HER2-Positive Breast Cancer: Results from the GEICAM/2006-14 Trial. *Br. J. Cancer* **2014**, *110* (5), 1139–1147.
- (105) Kato, K.; Takahashi, S.; Cui, L.; Toda, T.; Suzuki, S.; Futakuchi, M.; Sugiura, S.; Shirai, T. Suppressive Effects of Dietary Genistin and Daidzin on Rat Prostate Carcinogenesis. *Jpn. J. Cancer Res.* **2000**, *91* (8), 786–791.
- (106) Pendyala, B.; Patras, A. In Silico Screening of Food Bioactive Compounds to Predict Potential Inhibitors of COVID-19 Main Protease (Mpro) and RNA-Dependent RNA Polymerase (RdRp). **2020**.
- (107) Sharp, K.; Dange, D.; others. Computational Drug Simulation: A Step to the Possible Cure of COVID-19. **2020**.
- (108) Ekholm, S.; Foley, M.; Kido, D.; Morris, T. Lumbar Myelography with Metrizamide in Rabbits: An Investigation of Contrast Media Penetration and Resorption. *Acta Radiol. Diagn. (Stockh.)* **1984**, *25* (6), 517–522.
- (109) Kudo, S.; Ishizaki, T. Pharmacokinetics of Haloperidol. *Clin. Pharmacokinet.* **1999**, *37* (6), 435–456.
- (110) Schuckit, M. A. Recognition and Management of Withdrawal Delirium (Delirium Tremens). *N. Engl. J. Med.* **2014**, *371* (22), 2109–2113.
- (111) Thorn, C. F.; Aklilu, E.; McDonagh, E. M.; Klein, T. E.; Altman, R. B. PharmGKB Summary: Caffeine Pathway. *Pharmacogenet. Genomics* **2012**, *22* (5), 389.
- (112) Day, M. Covid-19: Ibuprofen Should Not Be Used for Managing Symptoms, Say Doctors and Scientists; British Medical Journal Publishing Group, 2020.
- (113) FitzGerald, G. A. Misguided Drug Advice for COVID-19. *Science* **2020**, *367* (6485), 1434–1436.
- (114) Fan, E.; Merritt, E. A.; Zhang, Z.; Pickens, J. C.; Roach, C.; Ahn, M.; Hol, W. G. Exploration of the GM1 Receptor-Binding Site of Heat-Labile Enterotoxin and Cholera Toxin by Phenyl-Ring-Containing Galactose Derivatives. *Acta Crystallogr. D Biol. Crystallogr.* **2001**, *57* (2), 201–212.
- (115) Thanapongsathorn, W.; Vajrabukka, T. Clinical Trial of Oral Diosmin (Daflon®) in the Treatment of Hemorrhoids. *Dis. Colon Rectum* **1992**, *35* (11), 1085–1088.
- (116) Feroso, J.; Legido, A. G.; Del Pino, J.; Valiente, R. Therapeutic Value of Hidrosmin in the Treatment of Venous Disorders of the Lower Limbs. *Curr. Ther. Res.* **1992**, *52* (1), 124–134.
- (117) Meneguzzo, F.; Ciriminna, R.; Zabini, F.; Pagliaro, M. Accelerated Production of Hesperidin-Rich Citrus Pectin from Waste Citrus Peel for Prevention and Therapy of COVID-19. **2020**.
- (118) Nabirotkin, S.; Peluffo, A. E.; Bouaziz, J.; Cohen, D. Focusing on the Unfolded Protein Response and Autophagy Related Pathways to Reposition Common Approved Drugs against COVID-19. **2020**.

- (119) Pinkosky, S. L.; Newton, R. S.; Day, E. A.; Ford, R. J.; Lhotak, S.; Austin, R. C.; Birch, C. M.; Smith, B. K.; Filippov, S.; Groot, P. H.; others. Liver-Specific ATP-Citrate Lyase Inhibition by Bempedoic Acid Decreases LDL-C and Attenuates Atherosclerosis. *Nat. Commun.* **2016**, 7 (1), 1–13.
- (120) Caly, L.; Druce, J. D.; Catton, M. G.; Jans, D. A.; Wagstaff, K. M. The FDA-Approved Drug Ivermectin Inhibits the Replication of SARS-CoV-2 in Vitro. *Antiviral Res.* **2020**, 104787.
- (121) Mastrangelo, E.; Pezzullo, M.; De Burghgraeve, T.; Kaptein, S.; Pastorino, B.; Dallmeier, K.; de Lamballerie, X.; Neyts, J.; Hanson, A. M.; Frick, D. N.; others. Ivermectin Is a Potent Inhibitor of Flavivirus Replication Specifically Targeting NS3 Helicase Activity: New Prospects for an Old Drug. *J. Antimicrob. Chemother.* **2012**, 67 (8), 1884–1894.
- (122) Spitsin, S.; Hooper, D.; Leist, T.; Streletz, L.; Mikheeva, T.; Koprowski, H. Inactivation of Peroxynitrite in Multiple Sclerosis Patients after Oral Administration of Inosine May Suggest Possible Approaches to Therapy of the Disease. *Mult. Scler. J.* **2001**, 7 (5), 313–319.
- (123) Svedmyr, N. Fenoterol: A Beta2-Adrenergic Agonist for Use in Asthma; Pharmacology, Pharmacokinetics, Clinical Efficacy and Adverse Effects. *Pharmacother. J. Hum. Pharmacol. Drug Ther.* **1985**, 5 (3), 109–126.
- (124) Kahn, J. O.; Lagakos, S. W.; Richman, D. D.; Cross, A.; Pettinelli, C.; Liou, S.; Brown, M.; Volberding, P. A.; Crumpacker, C. S.; Beall, G.; others. A Controlled Trial Comparing Continued Zidovudine with Didanosine in Human Immunodeficiency Virus Infection. *N. Engl. J. Med.* **1992**, 327 (9), 581–587.
- (125) Alakwaa, F. M. Repurposing Didanosine as a Potential Treatment for COVID-19 Using Single-Cell RNA Sequencing Data. *Msystems* **2020**, 5 (2).
- (126) Bukreyeva, N.; Mantlo, E. K.; Sattler, R. A.; Huang, C.; Paessler, S.; Zeldis, J. The IMPDH Inhibitor Merimepodib Suppresses SARS-CoV-2 Replication in Vitro. *bioRxiv* **2020**.
- (127) McLaren, C.; Datema, R.; Knupp, C.; Buroker, R. Didanosine. *Antivir. Chem. Chemother.* **1991**, 2 (6), 321–328.
- (128) Klimke, A.; Hefner, G.; Will, B.; Voss, U. Hydroxychloroquine as an Aerosol Might Markedly Reduce and Even Prevent Severe Clinical Symptoms after SARS-CoV-2 Infection. *Med. Hypotheses* **2020**, 109783.
- (129) Moskal, M.; Beker, W.; Roszak, R.; Gajewska, E. P.; Wołos, A.; Molga, K.; Szymkuć, S.; Grzybowski, B. A. Suggestions for Second-Pass Anti-COVID-19 Drugs Based on the Artificial Intelligence Measures of Molecular Similarity, Shape and Pharmacophore Distribution. **2020**.
- (130) Schaaf, L.; Dobbs, B.; Edwards, I.; Perrier, D. The Pharmacokinetics of Doxifluridine and 5-Fluorouracil after Single Intravenous Infusions of Doxifluridine to Patients with Colorectal Cancer. *Eur. J. Clin. Pharmacol.* **1988**, 34 (5), 439–443.
- (131) Zhang, Z.-F.; Fan, S.-H.; Zheng, Y.-L.; Lu, J.; Wu, D.-M.; Shan, Q.; Hu, B. Troxerutin Improves Hepatic Lipid Homeostasis by Restoring NAD⁺-Depletion-Mediated Dysfunction of Lipin 1 Signaling in High-Fat Diet-Treated Mice. *Biochem. Pharmacol.* **2014**, 91 (1), 74–86.
- (132) Mittal, L.; Kumari, A.; Srivastava, M.; Singh, M.; Asthana, S. Identification of Potential Molecules against COVID-19 Main Protease through Structure-Guided Virtual Screening Approach. **2020**.
- (133) Liu, X.-Y. Therapeutic Effect of Chai-Ling-Tang (Sairei-to) on the Steroid-Dependent Nephrotic Syndrome in Children. *Am. J. Chin. Med.* **1995**, 23 (03n04), 255–260.
- (134) Yang, L.; Li, Y.-T.; Miao, J.; Wang, L.; Fu, H.; Li, Q.; Wen, W.-B.; Zhang, Z.-Y.; Song, R.-W.; Liu, X.-G.; others. Network Pharmacology Studies on the Effect of Chai-Ling Decoction in Coronavirus Disease 2019. *Tradit. Med. Res.* **2020**, 5 (3), 145–159.

- (135) Brayer, G. D.; Sidhu, G.; Maurus, R.; Rydberg, E. H.; Braun, C.; Wang, Y.; Nguyen, N. T.; Overall, C. M.; Withers, S. G. Subsite Mapping of the Human Pancreatic α -Amylase Active Site through Structural, Kinetic, and Mutagenesis Techniques. *Biochemistry* **2000**, 39 (16), 4778–4791.
- (136) Elson-Schwab, L.; Tor, Y. Targeting HIV-1 RNA with Aminoglycoside Antibiotics and Their Derivatives. *Aminoglycoside Antibiot.* **2007**, 267–287.
- (137) Weissmann, B.; Meyer, K. The Structure of Hyalobiuronic Acid and of Hyaluronic Acid from Umbilical Cord1, 2. *J. Am. Chem. Soc.* **1954**, 76 (7), 1753–1757.
- (138) Stauder, G.; Ransberger, K. *Treatment of Hepatitis C Virus Infection Using a Protease and a Flavonoid*; Google Patents, 2001.
- (139) Sanford, M.; Plosker, G. L. Anastrozole. *Drugs* **2008**, 68 (9), 1319–1340.
- (140) Lønning, P. E. Clinical Pharmacokinetics of Aromatase Inhibitors and Inactivators. *Clin. Pharmacokinet.* **2003**, 42 (7), 619–631.
- (141) Stakheev, D.; Taborska, P.; Strizova, Z.; Podrazil, M.; Bartunkova, J.; Smrz, D. The WNT/ β -Catenin Signaling Inhibitor XAV939 Enhances the Elimination of LNCaP and PC-3 Prostate Cancer Cells by Prostate Cancer Patient Lymphocytes in Vitro. *Sci. Rep.* **2019**, 9 (1), 1–14.
- (142) Grunewald, M. E.; Chen, Y.; Kuny, C.; Maejima, T.; Lease, R.; Ferraris, D.; Aikawa, M.; Sullivan, C. S.; Perlman, S.; Fehr, A. R. The Coronavirus Macrodome Is Required to Prevent PARP-Mediated Inhibition of Virus Replication and Enhancement of IFN Expression. *PLoS Pathog.* **2019**, 15 (5).
- (143) Alhammad, Y. M.; Fehr, A. R. The Viral Macrodome Counters Host Antiviral ADP-Ribosylation. *Viruses* **2020**, 12 (4), 384.
- (144) Khalatbari-mohseni, A.; Banafshe, H. R.; Mirhosseini, N.; Asemi, Z.; Ghaderi, A.; Omid, A. The Effects of Crocin on Psychological Parameters in Patients under Methadone Maintenance Treatment: A Randomized Clinical Trial. *Subst. Abuse Treat. Prev. Policy* **2019**, 14 (1), 9.
- (145) di Camillo Orfali, G.; Duarte, A. C.; Bonadio, V.; Martinez, N. P.; De Araújo, M. E. M. B.; Priviero, F. B. M.; Carvalho, P. O.; Priolli, D. G. Review of Anticancer Mechanisms of Isoquercetin. *World J. Clin. Oncol.* **2016**, 7 (2), 189.
- (146) Gane, E. J.; Rouzier, R.; Wiercinska-Drapalo, A.; Larrey, D. G.; Morcos, P. N.; Brennan, B. J.; Le Pogam, S.; Nájera, I.; Petric, R.; Tran, J. Q.; others. Efficacy and Safety of Danoprevir-Ritonavir plus Peginterferon Alfa-2a-Ribavirin in Hepatitis C Virus Genotype 1 Prior Null Responders. *Antimicrob. Agents Chemother.* **2014**, 58 (2), 1136–1145.
- (147) Sekhar, T. *Virtual Screening Based Prediction of Potential Drugs for COVID-19*; Preprints, 2020.
- (148) Chen, H.; Zhang, Z.; Wang, L.; Huang, Z.; Gong, F.; Li, X.; Chen, Y.; others. First Clinical Study Using HCV Protease Inhibitor Danoprevir to Treat Naive and Experienced COVID-19 Patients. *medRxiv* **2020**.
- (149) Johnson, C. A.; Zimmerman, S.; Reitberg, D.; Whall, T.; Leggett, J.; Craig, W. Pharmacokinetics and Pharmacodynamics of Cefoperazone-Sulbactam in Patients on Continuous Ambulatory Peritoneal Dialysis. *Antimicrob. Agents Chemother.* **1988**, 32 (1), 51–56.
- (150) Zhang, G.; Hu, C.; Luo, L.; Fang, F.; Chen, Y.; Li, J.; Peng, Z.; Pan, H. Clinical Features and Outcomes of 221 Patients with COVID-19 in Wuhan, China. *MedRxiv* **2020**.
- (151) Li, Y.; Zhao, R.; Zheng, S.; Chen, X.; Wang, J.; Sheng, X.; Zhou, J.; Cai, H.; Fang, Q.; Yu, F.; others. Early Release-Lack of Vertical Transmission of Severe Acute Respiratory Syndrome Coronavirus 2, China. **2020**.
- (152) Ena, J.; Amador, C.; Benito, C.; Pasquau, F. Pharmacological and Clinical Evidence of Nevirapine Immediate-and Extended-Release Formulations. *HIVAIDS Auckl. NZ* **2012**, 4, 169.

- (153) Kadioglu, O.; Saeed, M.; Johannes Greten, H.; Efferth, T. Identification of Novel Compounds against Three Targets of SARS CoV-2 Coronavirus by Combined Virtual Screening and Supervised Machine Learning.
- (154) Lee, V. S.; Chong, W. L.; Sukumaran, S. D.; Nimmanpipug, P.; Letchumanan, V.; Goh, B. H.; Lee, L.-H.; Zain, S. M.; Abd Rahman, N. Computational Screening and Identifying Binding Interaction of Anti-Viral and Anti-Malarial Drugs: Toward the Potential Cure for SARS-CoV-2. *Prog. Drug Discov. Biomed. Sci.* **2020**, 3 (1).
- (155) Andritsos, L. A.; Dunavin, N.; Lozanski, G.; Jones, J. A.; Blachly, J. S.; Lucas, D. M.; Byrd, J. C.; Kraut, E.; Grever, M. R. Reduced Dose Pentostatin for Initial Management of Hairy Cell Leukemia Patients Who Have Active Infection or Risk of Hemorrhage Is Safe and Effective. *haematologica* **2014**, haematol-2014.
- (156) Zhang, L.; Zhou, R. Binding Mechanism of Remdesivir to SARS-CoV-2 RNA Dependent RNA Polymerase. **2020**.
- (157) Wishart, D. S. DrugBank: A General Resource for Pharmaceutical and Pharmacological Research. *Mol. Cell. Pharmacol.* **2010**, 2 (1), 25–38.

FIGURE AND TABLE LEGENDS

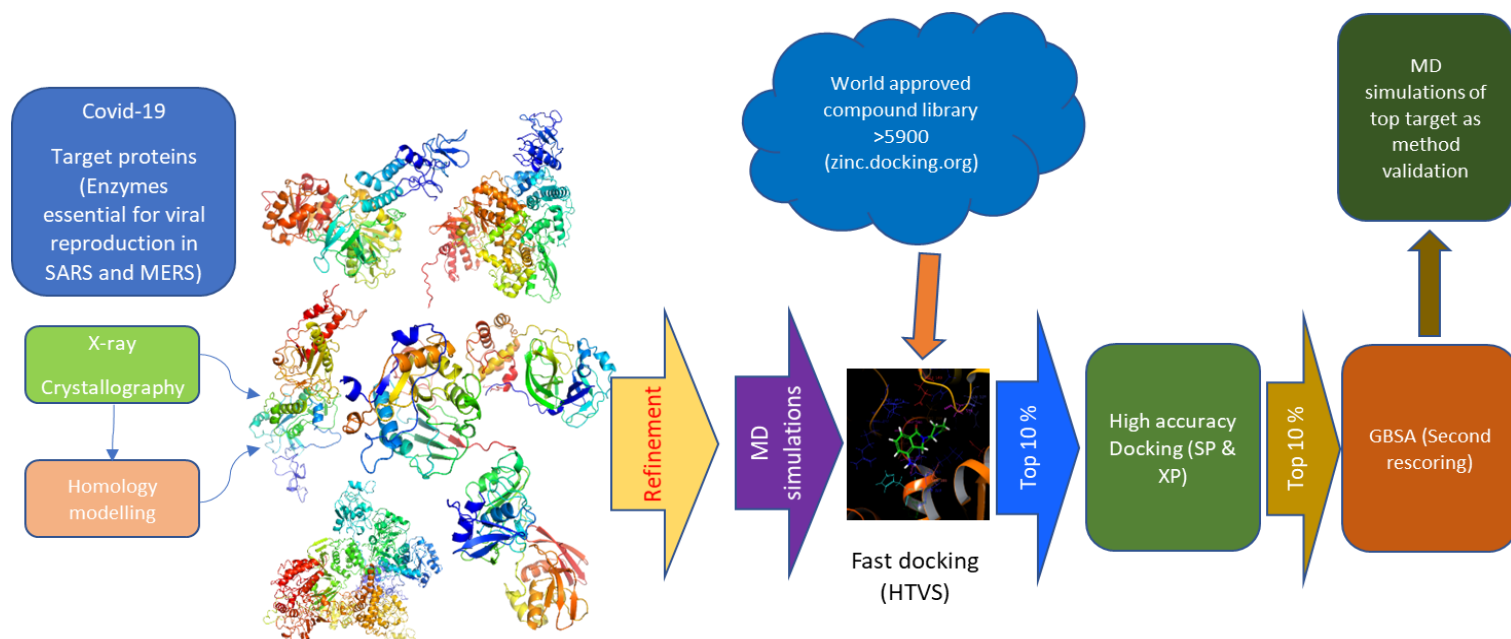


Fig 1. Schematic road map of the overall study design. The protein models from various protein bank and other sources were optimized and relaxed by MD simulations. The relaxed structures were then mapped for active site and used to generate GLIDE Grid for HT-virtual screen with world approved drug libraries.

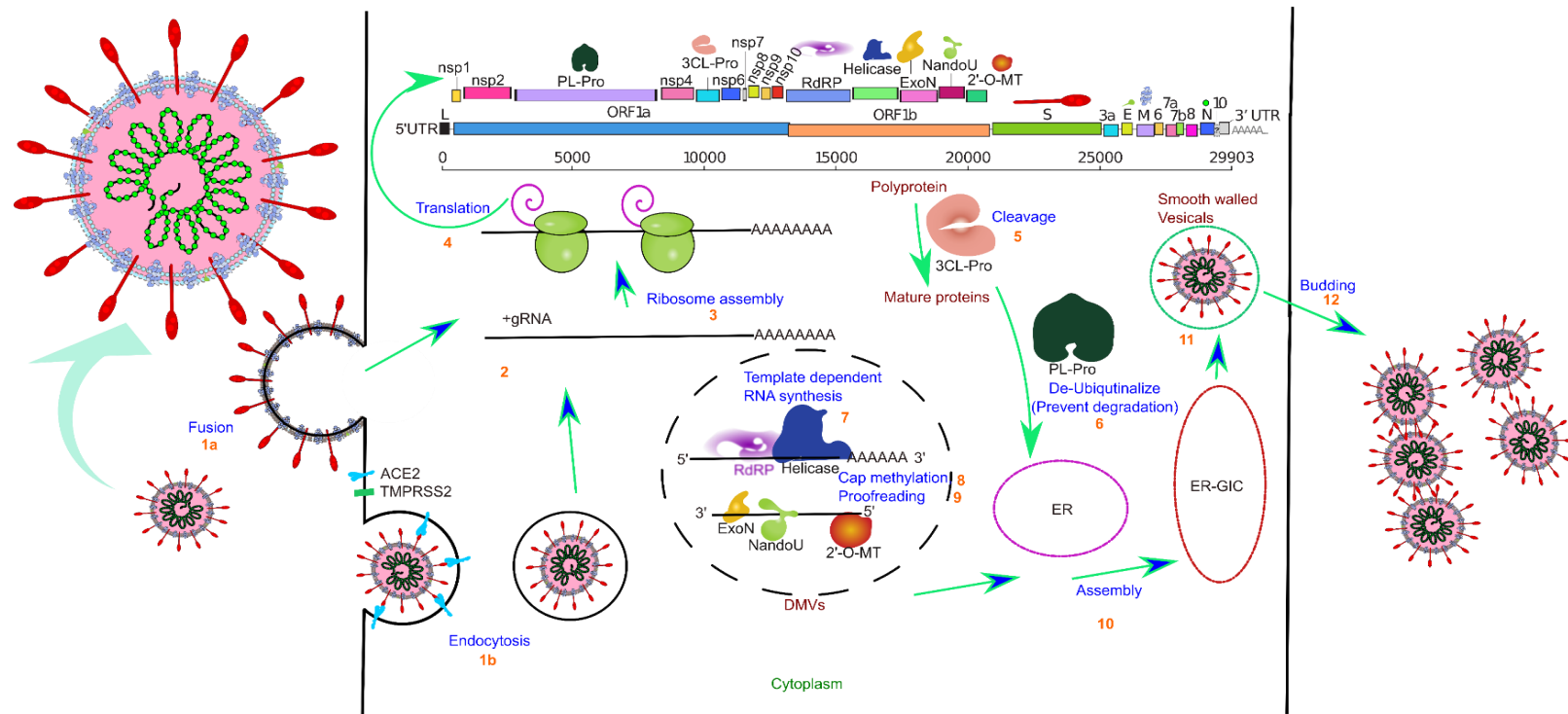


Fig 2. Graphical illustration of SARS-CoV-2 life cycle along with target proteins used in HTVS. The infection cycle starts when SARS-CoV-2 Spike protein binds to the Human ACE2 receptor. An S1-induced post-stable S2 conformation allows either viral-host cell fusion (1a) or endocytosis (1b). Fusion directly allows the viral RNA to enter the host cell (2), but endocytosis require lysosomal degradation of coat and envelop for release of viral nucleocapsid in cytoplasm. The large viral script is known to encode 29 viral proteins (3), including the 7 essential nonstructural proteins that are selected as targets in our paper. A replicase is used to translate most of the viral genomic RNA to synthesize two replicase polyproteins, pp1a and pp1ab, and many small ORFs(4). The two major polyproteins are processed by two proteases, PLpro and 3CLpro(5), generating 16 nonstructural proteins. ExoN possesses a viral exoribonuclease activity that acts on both ssRNA and dsRNA in a 3' to 5' direction(9). Viral Helicase plays a critical role in viral replication by expediting appropriate folding (7). The enzyme 2'-O-MT methylates the viral 2' end which is important for the virion to avoid host recognition of their RNA (8). RdRp is involved in viral-host cell replication through catalyzing template synthesis of polynucleotides in the 5' to 3' direction (7). NandoU is a Mn^{2+} dependent hexamer (dimer of trimer) enzyme with sparse functional information. The most prominent theory regarding NandoU is that the activity of this protein is responsible for protein interference with the innate immune system. For viral assembly of S, E and M proteins in the endoplasmic reticulum, along with the N protein are combined with the (+) gRNA to become a helical nucleoprotein complex. They assemble to form a virus particle in the endoplasmic reticulum-Golgi apparatus compartment, this particle is then excreted from cell through exocytosis within the smooth vesicles.

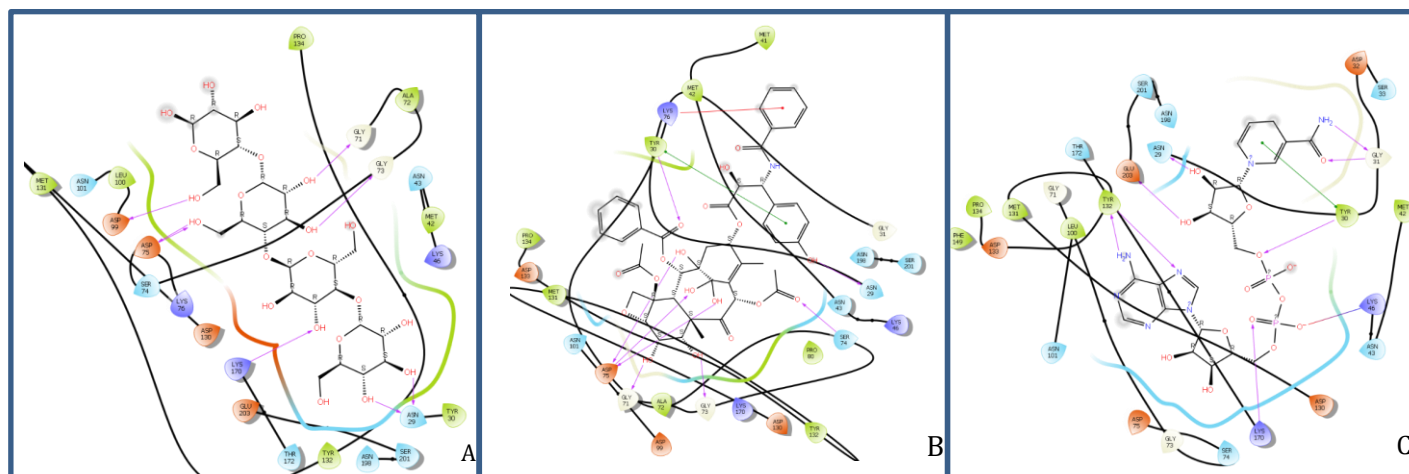


Fig 3. 2D Ligand interaction maps of the top 3 hits (**Table3**) within the **2'-O-methyltransferase (2'-O-MT)** binding pocket (Schrödinger LLC_2020-1) depicting amino acid side chain residues colored according to their biochemical nature i.e. red = acidic, violet = basic, green = hydrophilic, and light blue = hydrophobic. The bold lines depict peptide backbone and red arrows depict molecular interactions.

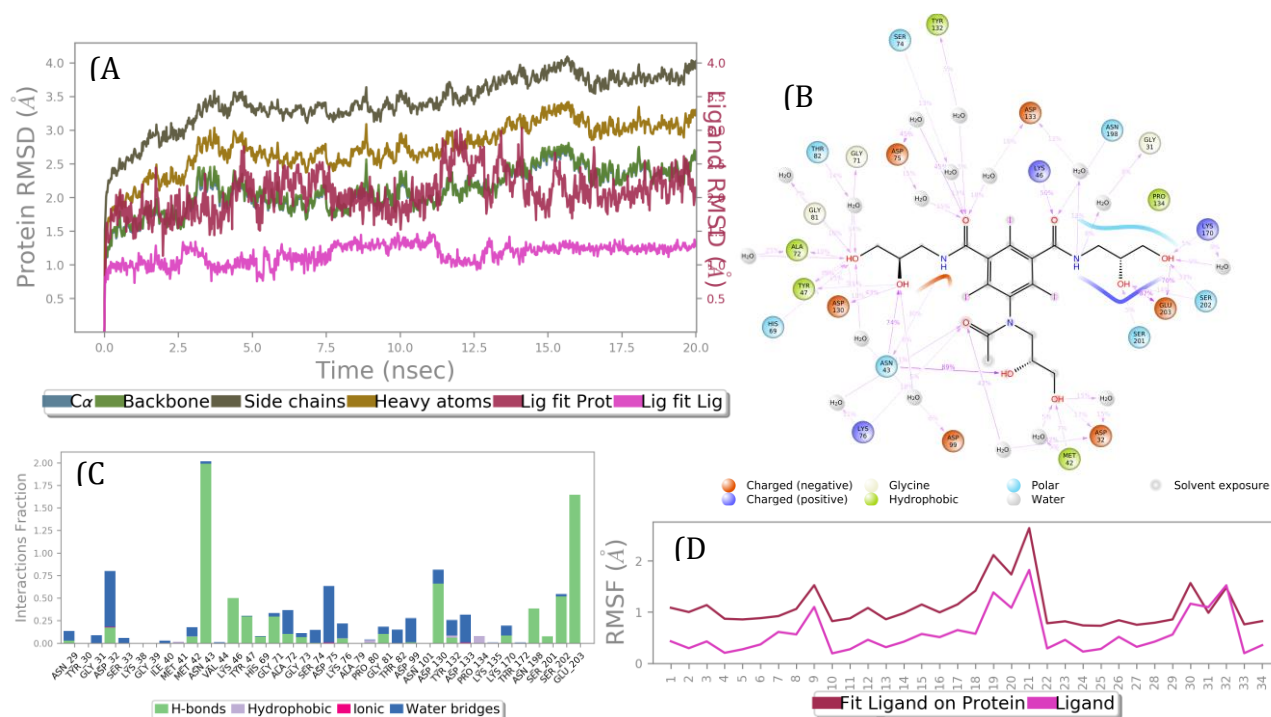


Fig 4. Results of a 20 ns MD simulation (A) Root mean square deviations difference between the 2'-O-methyltransferase (2'-O-MT) and the bound ligand iohecol. Graph obtained for RMSF values of ligand (purple line) from the protein back bone (green line). The ligand remained in the bound state throughout the simulation. (B) Schematic 2D representation of bound ligand interactions of iohecol throughout the simulation. (C) Critical protein ligand contacts of amino acid sidechain residues with the interaction properties (D) Root mean square fluctuations between the binding site of target protein and the interacting ligand.

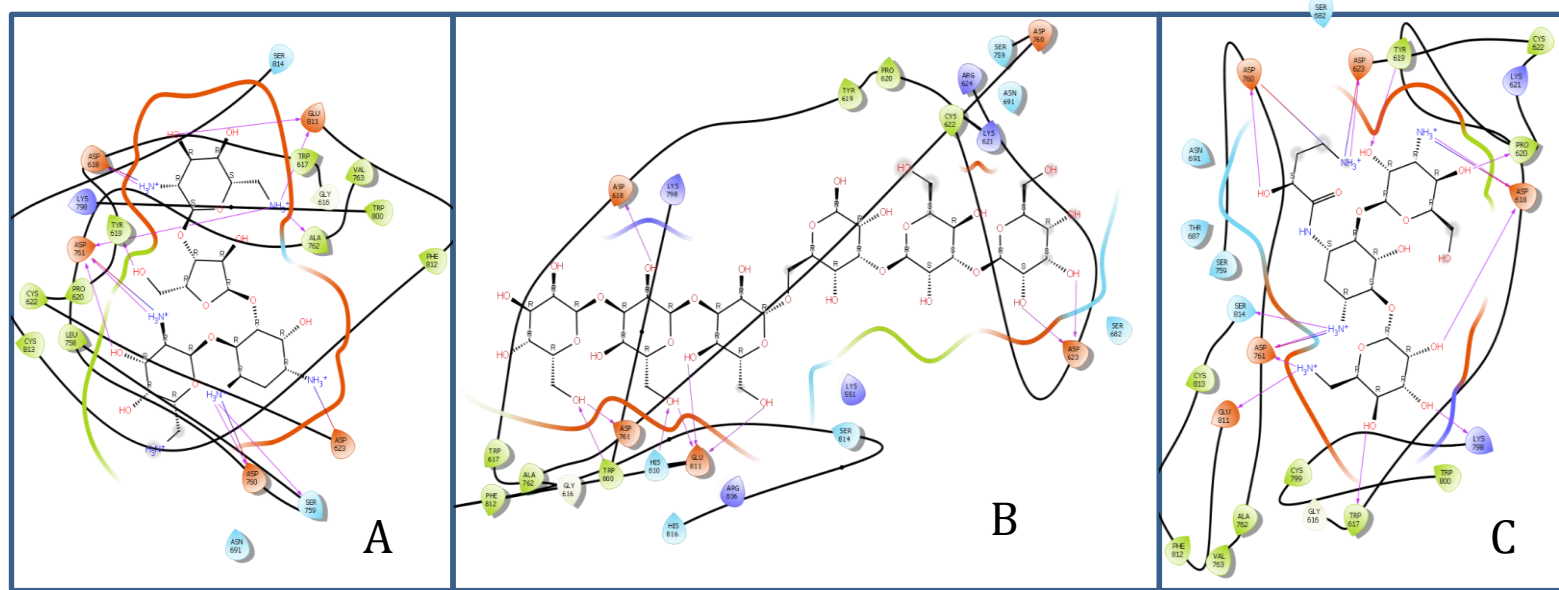


Fig 5. 2D Ligand interaction maps of the top 3 hits (Table4) within RdRP (RNA-dependent RNA polymerase) binding pocket (Schrödinger, 2020-1) depicting amino acid side chain residues colored according to their biochemical nature i.e. red = acidic, violet = basic, green = hydrophilic, and light blue = hydrophobic. bold lines depict peptide backbone and red arrows depict molecular interactions.

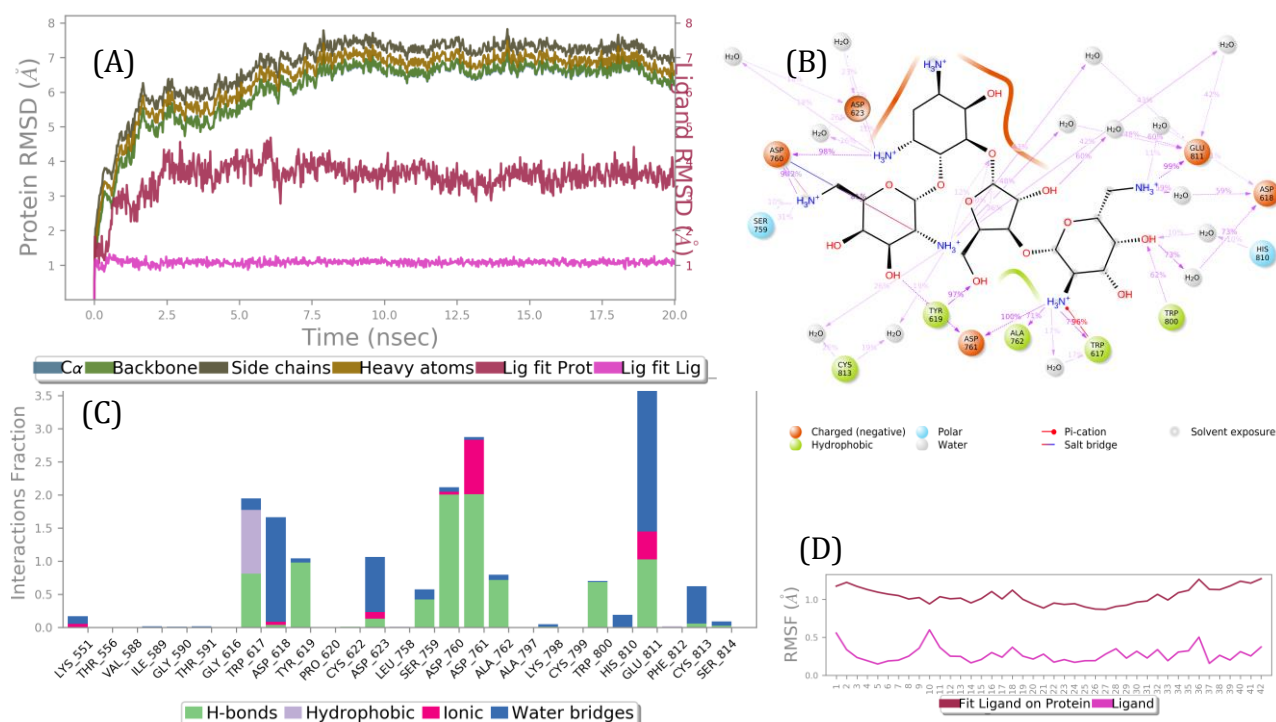


Fig 6. Results of a 20 ns MD simulation. (A) Root mean square deviations (RMSD) differences between the RNA-directed RNA polymerase (RdRp) and the bound ligand paromomycin, with the graph obtained for the RMSF value of ligand (purple line) from the protein back bone (green line). The entire ligand is involved in a very strong binding, and there was little movement observed for the ligand throughout the simulation period. (B) The acidic amino acid side 2D interaction map of bound paromomycin interactions throughout the simulation. (C) Critical protein-ligand contacts of amino acid side chain residues with the interaction properties by type. (D) Root mean square fluctuations between the binding site of target protein and the interacting paromomycin ligand.

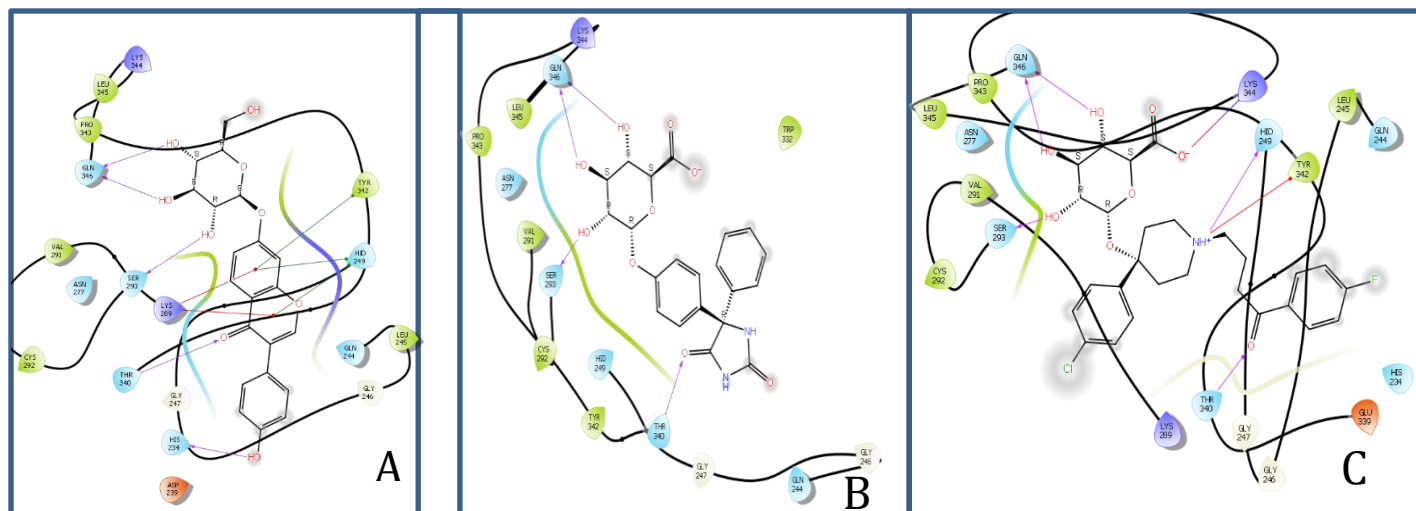


Fig.7. 2D Ligand interaction maps of the top 3 hits (Table 5): A) daidzin, B) phenytoin glucuronide, and C) haloperidol glucuronide within the **Uridylate-specific endoribonuclease (NendoU)** binding pocket as determined by (Schrödinger LLC_2020-1) depicting amino acid side chain residues colored according to their biochemical nature i.e. red = acidic, violet = basic, green = hydrophilic, and light blue = hydrophobic. The bold lines depict peptide backbone and red arrows depict molecular interactions. The bold lines depict peptide backbone and red arrows depict molecular interactions.

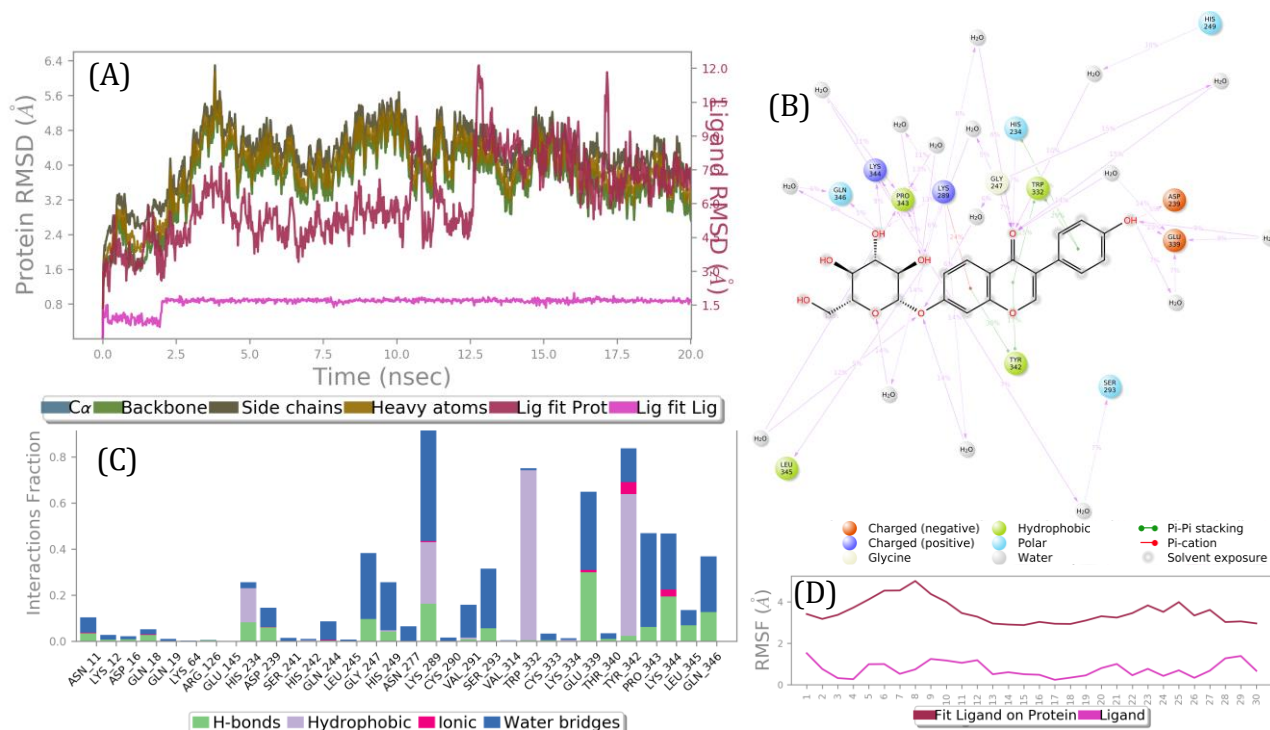


Fig 8. Results of a 20 ns MD simulation (A) Root mean square deviations (RMSD) differences between the Uridylate-specific endoribonuclease (NandoU) and bound ligand diadzin, with the graph obtained for RMSF value of ligand (purple line) from the protein back bone (green line). The ligand underwent major conformational changes with respect to its interactions with Trp-332 and Glu-339. The complex attained high stability within 12 ns and remained highly stable for the rest of the simulation. (B) The acidic amino acid side 2D interaction map of bound diadzin throughout the simulation. (C) Critical protein ligand contacts of amino acid side chain residues with the interaction properties (D) Root mean square fluctuations between the binding site of target protein and the diadzin ligand.

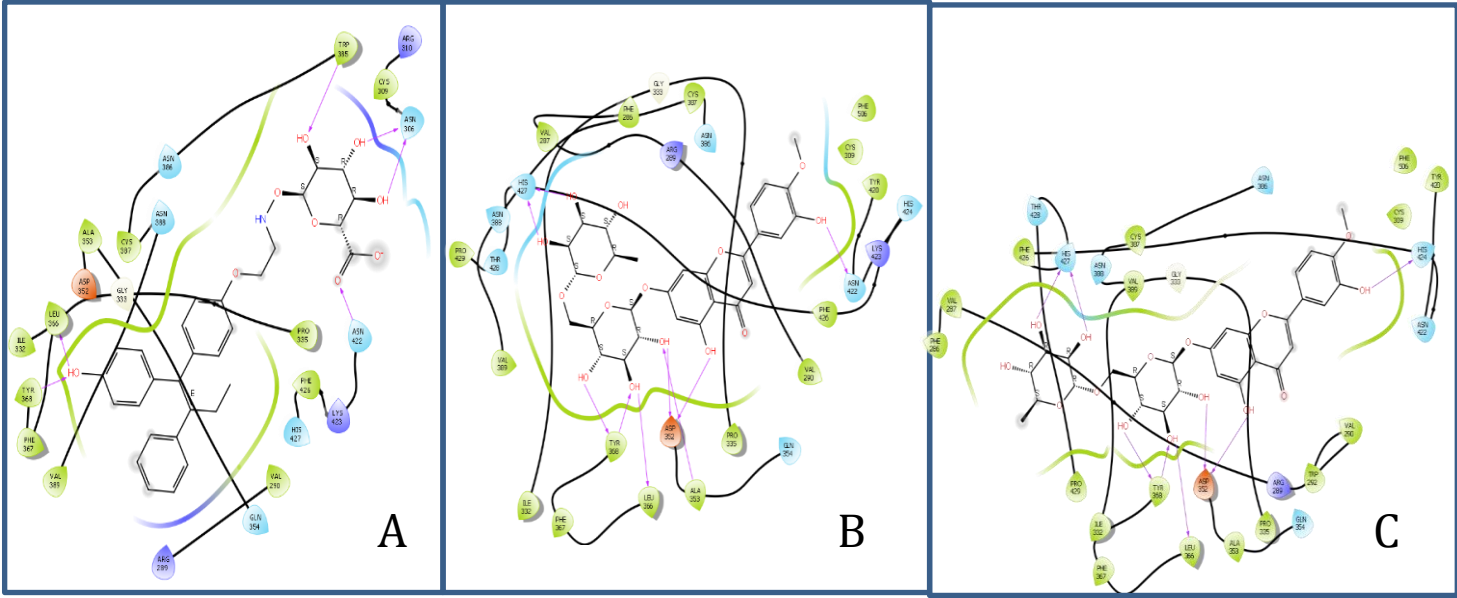


Fig 9. 2D Ligand interaction maps of the top 3 hits (Table 6) within the *Guanine-N7 methyltransferase (ExoN)* binding pocket (Schrödinger LLC_2020-1) depicting amino acid side chain residues colored according to their biochemical nature i.e. red = acidic, violet = basic, green = hydrophilic, and light blue = hydrophobic. The bold lines depict peptide backbone and red arrows depict molecular interactions.

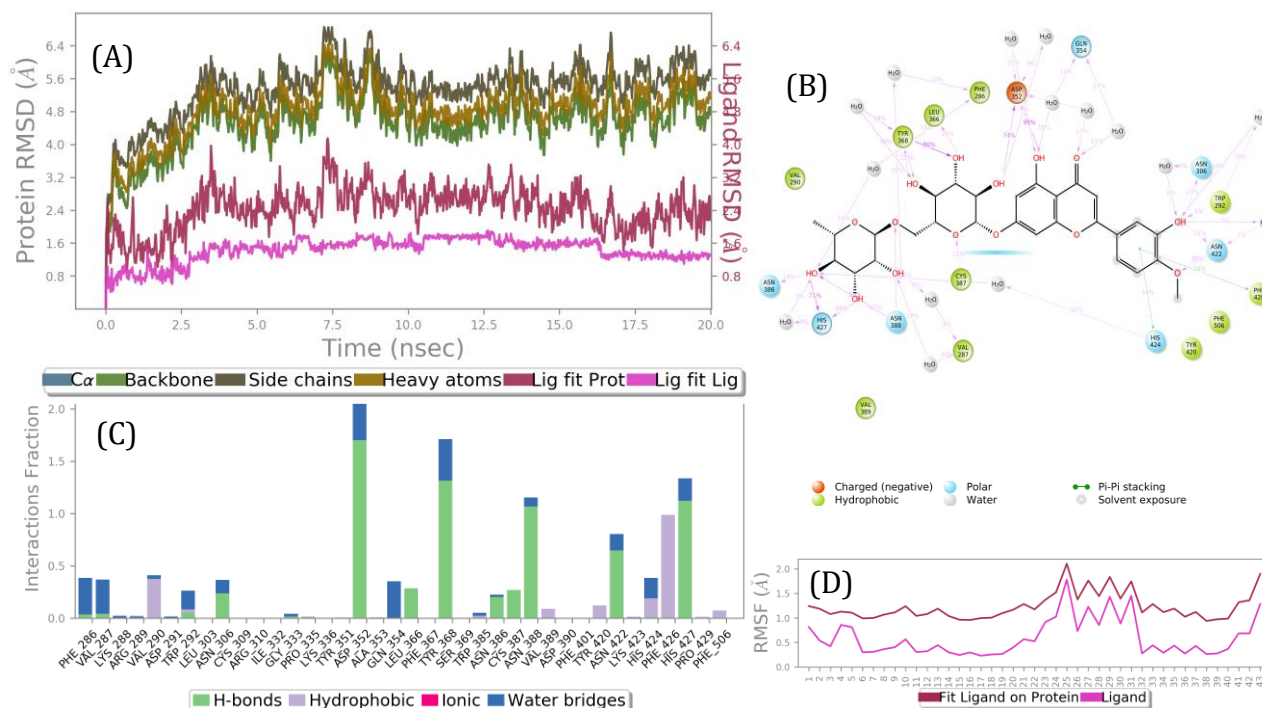


Fig 10. Results of a 20 ns MD simulation (A) Root mean square deviations difference between the guanine-N7 methyltransferase (ExoN) and bound ligand diosmin, with the graph obtained for RMSF value of ligand (purple line) from the protein back bone (green line), revealing that the ligand is very strongly bound to the active site of the target. (B) The acidic amino acid side 2D interaction map of bound diosmin throughout the simulation. (C) Critical protein ligand contacts of amino acid side chain residues with the interaction properties (D) Root mean square fluctuation between the binding site of target protein and interacting ligand.

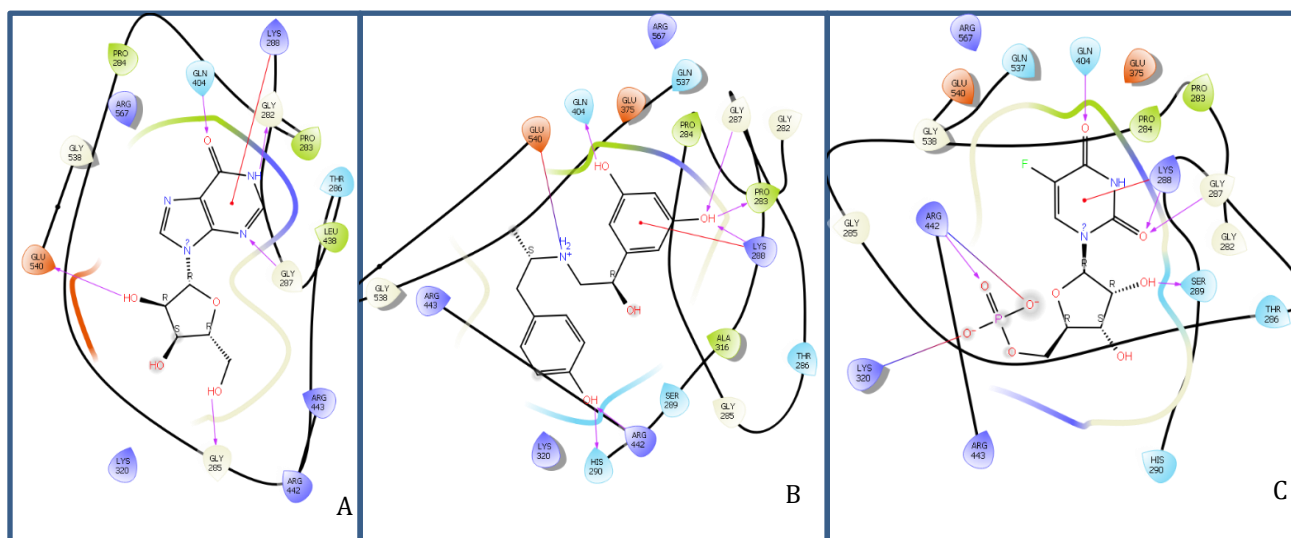


Fig.11. 2D Ligand interaction maps of the top 3 hits (Table 7) A) inosine, B) name, and C) 5-fluorouridine monophosphate within the **Helicase (Hel)** binding pocket (Schrödinger LLC_2020-1) depicting amino acid side chain residues colored according to their biochemical nature i.e. red = acidic, violet = basic, green = hydrophilic, and light blue = hydrophobic. The bold lines depict peptide backbone and red arrows depict molecular interactions.

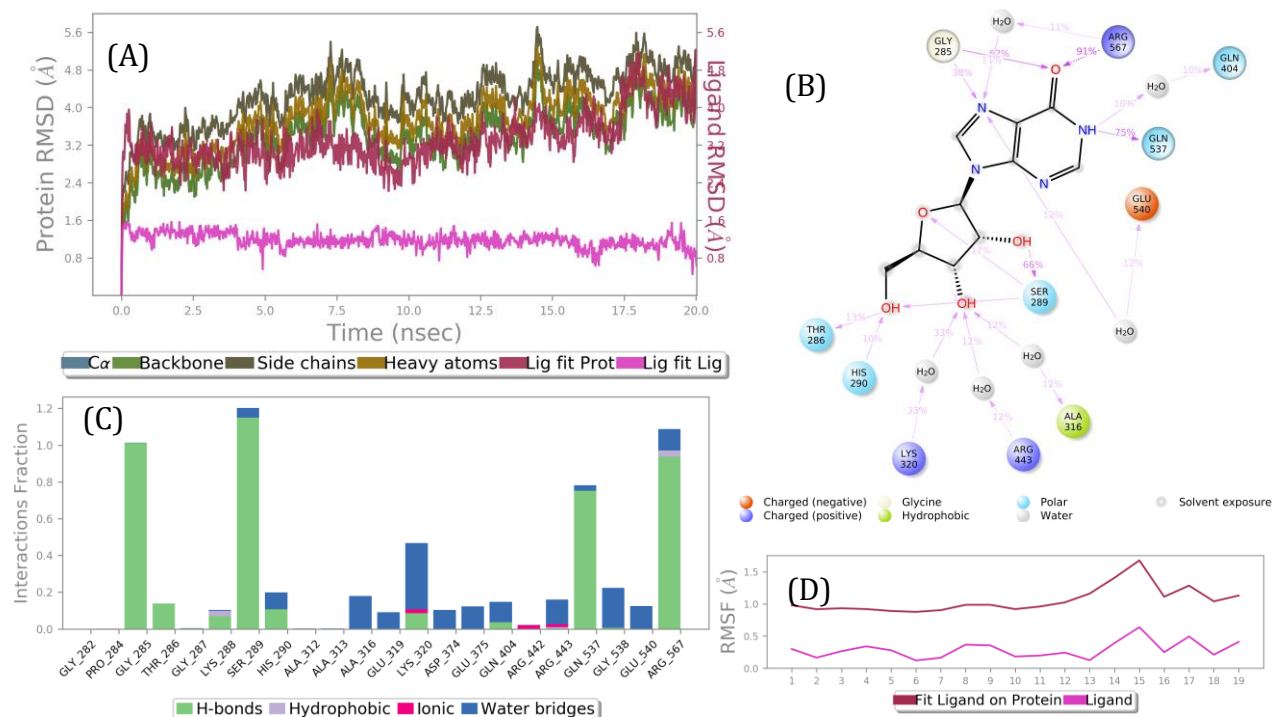


Fig 12. Results of a 20 ns MD simulation (A) Root mean square deviations difference between the Helicase and bound ligand inosine. Graph obtained for RMSF value of ligand (purple line) from the protein backbone (green line). The ligand was tightly bound to the ATP- unpaired nucleoside binding site. (B) The acidic amino acid side 2D interaction map of bound inosine throughout the simulation. (C) Critical protein ligand contacts of amino acid side chain residues with the interaction properties (D) Root mean square fluctuations between the binding site of target protein and interacting ligand.

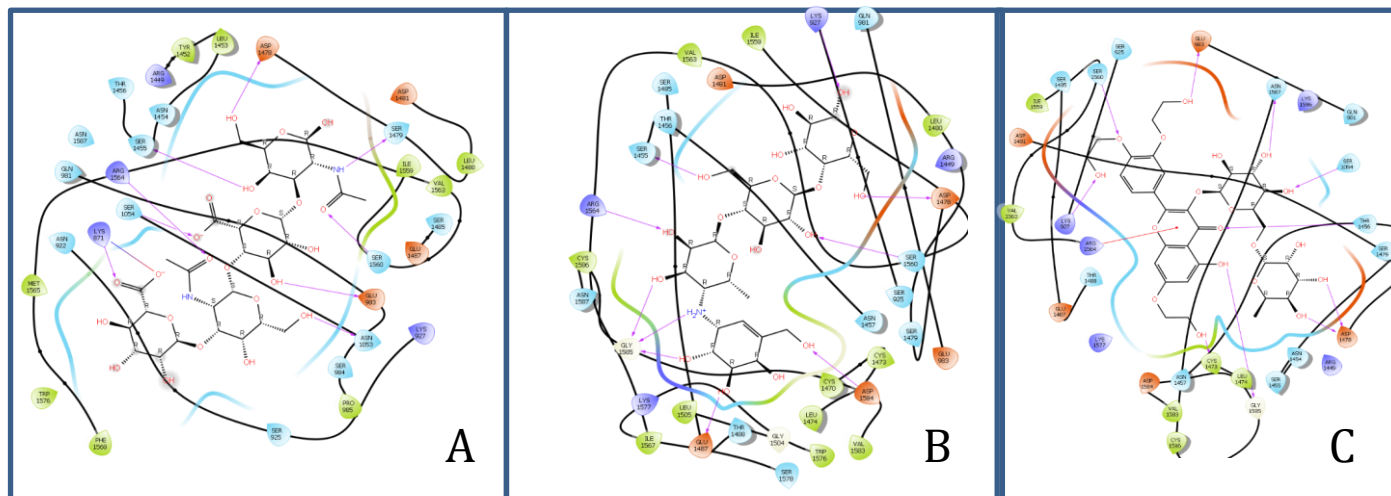


Fig 13. 2D Ligand interaction maps of the top 3 hits (Table 8) within *Papain-like proteinase (P1Pro)* binding pocket (Schrödinger LLC_2020-1) depicting amino acid side chain residues colored according to their biochemical nature i.e. red = acidic, violet = basic, green = hydrophilic, and light blue = hydrophobic. The bold lines depict peptide backbone and red arrows depict molecular interactions.

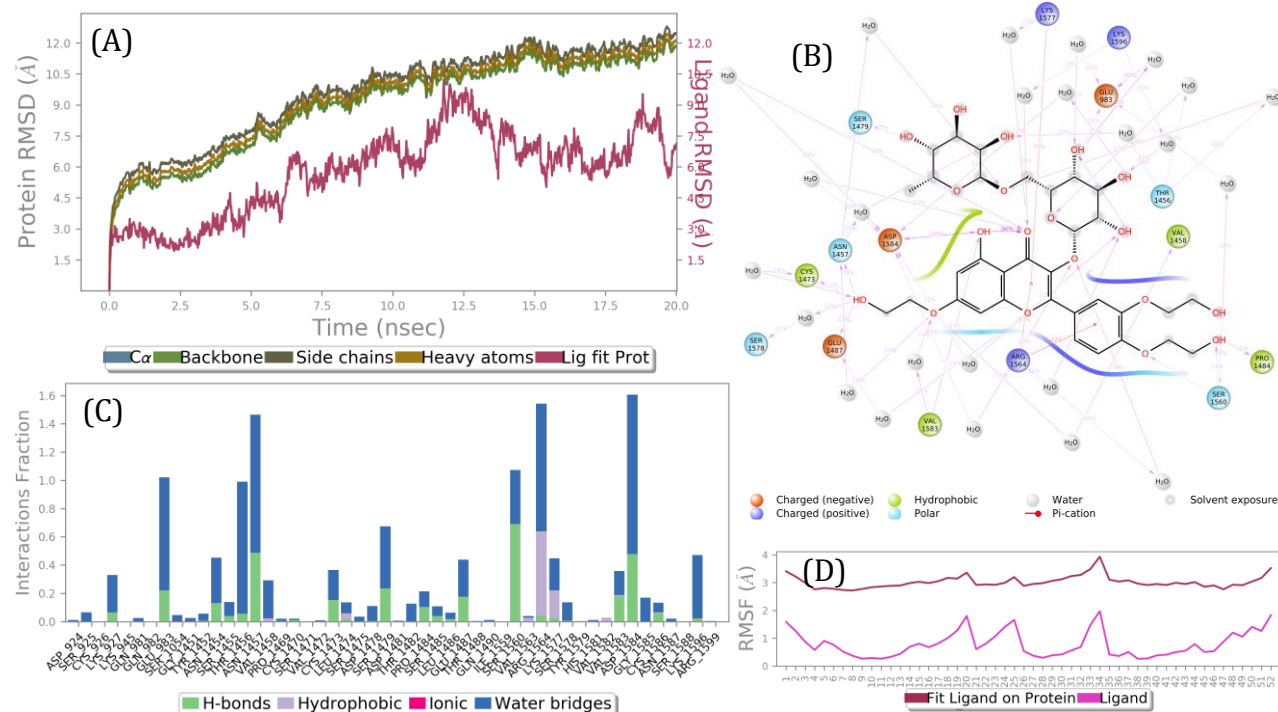


Fig 14. Results of a 20 ns MD simulation (A) Root mean square deviations difference between the Papain like protease (PlPro) and bound ligand troxerutin. Graph obtained for RMSF value of ligand (purple line) relative to the protein back bone (green line). The ligand was tightly bound to the de-ubiquitinylation site. (B) Schematic 2D representation of bound ligand interactions of Troxerutin throughout the simulation. (C) Critical protein ligand contacts of amino acid sidechain residues with the interaction properties (D) Root mean square fluctuation between the binding site of target protein and interacting ligand.

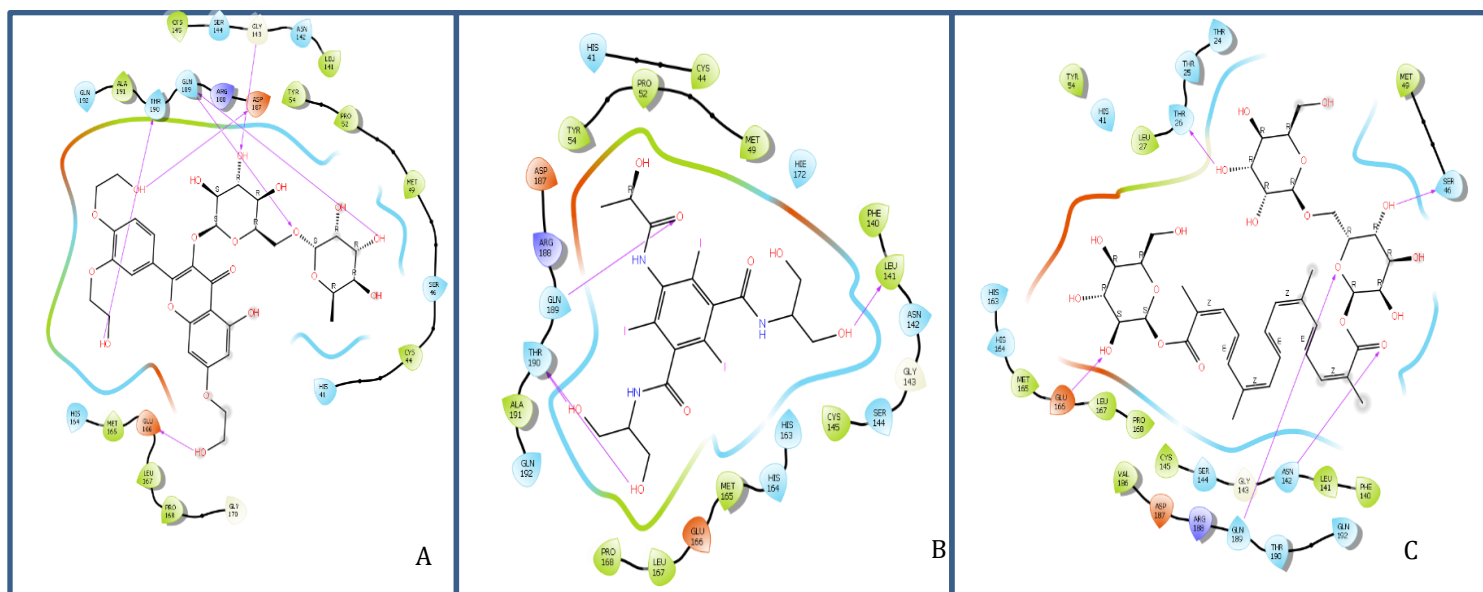


Fig 15. 2D Ligand interaction maps of the top 3 hits (Table 9) within the Main Proteinase (3CL-PRO) binding pocket (Schrödinger LLC_2020-1) depicting amino acid side chain residues colored according to their biochemical nature i.e. red = acidic, violet = basic, green = hydrophilic, and light blue = hydrophobic. The bold lines depict peptide backbone and red arrows depict molecular interactions.

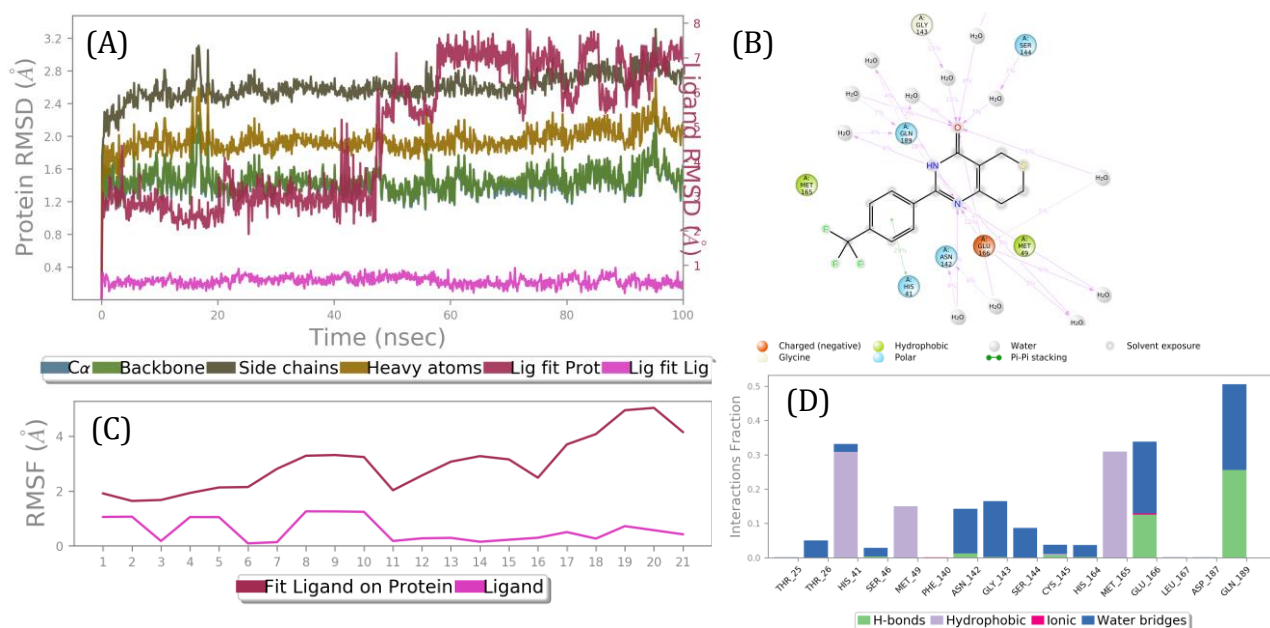


Fig 16. Results of a 20 ns MD simulation (A) Root mean square deviations difference between the Main protease (3CLPro) and bound ligand XAV-939. Graph obtained for RMSF value of ligand (purple line) from the protein back bone (green line). It revealed that there was a major conformational change of the ligand at around 50 ns without loss of the ligand. This suggests two binding conformers of same ligand within the binding site. (B) Schematic 2D representation of bound ligand interactions of XAV-939 throughout the simulation. (C) Root mean square fluctuation between the binding site of target protein and interacting ligand. (D) Critical protein ligand contacts of amino acid side chain residues with the interaction properties